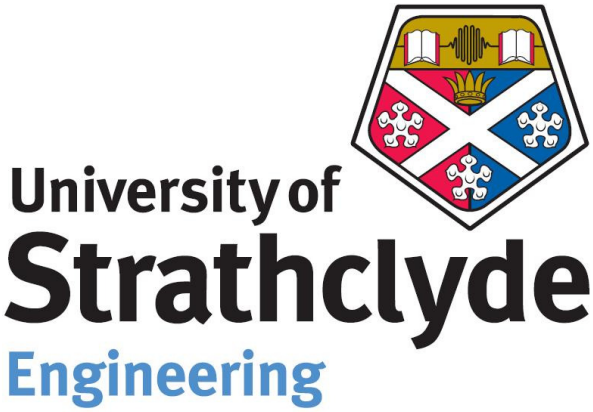

Department of Biomedical Engineering

The Design and Development of an Upper Limb Assistive Technology

Student: Stefan Di Donato

Supervisors: Dr. Heba Lakany & Dr. Wei Yao

A thesis presented in fulfilment of the requirements
for the degree of MSc Biomedical Engineering

August 2013

Declaration of Authenticity and Author's Rights

This thesis is the result of the author's original research. It has been composed by the author and has not been previously submitted for examination which has led to the award of a degree.

Stefan Di Donato

August 2013

Acknowledgements

First and foremost, thanks must go to my supervisors, Dr. Heba Lakany and Dr. Wei Yao for their guidance and support throughout this project.

Thanks must also be given to Mrs Radhika Menon for her assistance throughout the project, particularly in relation to the shape memory alloys and to Mrs Christine McMonagle from the National Centre of Prosthetics and Orthotics for her recommendations in the design.

Thanks to the staff of the Biomedical Engineering Unit for the taught portion of the MSc Biomedical Engineering course and to Mr Brian Cartlidge for all of his technical support.

Best wishes to my fellow classmates and friends on their completion of their MSc and to those undertaking their EngD course.

Finally, I must thank my family and friends back home in Australia for all of their encouragement throughout the year, with special thanks going to my parents and Jane for all of their support.

Abstract

Using modern robotic and biosignal integrated technologies; patients with limited upper limb mobility due to paresis, may finally have the opportunity to regain normal movement. An effective yet portable upper limb assistive orthosis has not yet been developed to rehabilitate these patients. A portable device would allow users to continue their rehabilitation without therapist supervision and work at their own pace.

This project aims to develop a working portable exoskeleton which assists flexion and extension of the elbow joint in patients who are unable to confidently move their arm. The elbow joint was chosen as it can be simplified to roughly one degree of freedom. The project will involve the design of the orthotic system using the modelling CAD software Pro|ENGINEER® while the mechanical analysis and simulation will be performed using MATLAB® Simulink.

In the future, the project will be expanded into the design and development of a full arm device which caters for shoulder mobility as well as hand and wrist assistance in order to provide complete rehabilitation and assistance to patients with very limited control of their upper limbs.

Table of Contents

List of Figures

List of Equations

List of Tables

Chapter 1: Introduction

1.1 Use of Orthotics in Rehabilitation

Every year, 15 million people around the world suffer from a stroke, according to the World Heart Federation and the National Stroke Association [1, 2]. Strokes are fatal for nearly six million of these people and of the eleven million survivors approximately 80 per cent suffer from hemiparesis. Kwakkel *et al.* [3] found that only 5 to 20 per cent of hemiplegic stroke victims had completely recovered after six months with a staggering 30 to 66 per cent regaining no function at all in the same time.

While stroke is one of the most debilitating injuries, there are other neurological conditions that can be improved with the use of upper limb physical therapy such as spinal cord injuries and damage to other neural pathways, sporting injuries and arthritis. Rehabilitation would serve to regain muscle strength, endurance and flexibility while reducing the pain caused by the disability.

Bayona *et al.* [4] discussed the importance of rehabilitation that is intensive, repetitive, task-specific, meaningful and challenging for patients. These factors are necessary for nerve damage patients in order to achieve long-lasting cortical reorganisation and the activation of damaged motor neuron pathways. Currently this training is provided manually by therapists although there have been steps towards using orthotics to assist in the recovery of patients' muscle strength and range of motion. While Tyson and Kent [5] showed that passive orthotics do not affect upper limb disability, range of movement and only potentially reduce pain development, Kwakkel *et al.* [6] described the interest in the integration of active, or powered orthotics for patient rehabilitation.

They discovered that powered physical therapy did not have any particular advantage at low utilisation over other forms of manual therapy, but showed that the benefits were noticeable when patients used the devices for longer periods. The robotic device allows patients to receive a more concentrated and consistent rehabilitation process while allowing therapists to reduce their workload. This reduced workload is achievable due to the fact that the patient is able to train by themselves, even in the privacy and comfort of their own homes. Wireless technology allows data to be communicated remotely from the device to therapists in order to monitor progress and ensure patient safety.

While robot-aided rehabilitation may not share the therapist's ability to adapt the patient's training regime instantaneously, it does offer reliable tools for the functional assessment of their progress such as changes in speed, direction, range of motion and strength. These devices can be made to function in assistive or resistive modes, allowing greater flexibility than standard rehabilitation tools in the modification of training regimes.

The fact that robotics can provide an effective and safe training procedure without the need for therapist supervision allows patients to work individually and at their own pace. This is one of the main reasons that these devices are being increasingly accepted by the rehabilitation community.

1.2 This Study

1.2.1 Motivation

Due to the fact that powered orthotics perform best during high intensity sessions that are conducted over long periods [6], it is important to have a comfortable device that patients can use independently. Current upper limb assistive technologies are generally mounted to chairs, workstations, tables or fixed to the ground. While this is adequate for patients restricted to wheelchairs if the device is portable, a design must be made which does not confine the patient to one location.

1.2.2 Aims and Objectives

The aim of this project is to develop the mechanical design of a light, portable and cheap upper limb orthosis which assists patients in elbow flexion and extension.

Using a set of requirements based on the literature, the device will be designed using the CAD software, Pro|ENGINEER® and optimised in terms of weight, power and range of motion. Once the design has been finalised, motion analysis will be conducted in terms of the kinematics and dynamics while a simulation of a functional device will be developed on MATLAB® Simulink.

Chapter 2: Literature Review

2.1 Advances in Rehabilitation Orthotics

While the use of passive upper limb orthotics is vital in the rehabilitation and treatment of many disabled patients, active orthotics are slowly becoming acknowledged as a powerful tool in the rehabilitation community due to their potential in improving the efficiency and effectiveness of training procedures. Tsagarakis and Caldwell [7] discussed in detail and systematically reviewed the recent advances in current powered orthotic technologies. They noted that while lower limb rehabilitation had an increasingly large and well regarded range of mechanical assistive products, upper arm rehabilitation was trailing behind with very few assistive devices available for patients.

2.1.1 Previous Designs

One of the earliest devices to be adopted was the Balanced Forearm Orthosis (BFO), a wheelchair based passive device designed in 1965 to assist in horizontal planar movement only. It was later modified to allow vertical movement but due to poor gravity compensation techniques the device was rarely used [8]. Another wheelchair mounted device, the Hybrid Arm Orthosis (HAO) developed by Benjuya and Kenney [9] assisted with shoulder abduction, elbow flexion, wrist supination, and came equipped with grasping assistance using three joint pinchers. It was controlled using a range of body movements, such as sip and puff switches and tongue switches though users did consider these control methods cumbersome and inadequate.

In 1992, the MIT-MANUS, a table-mounted rehabilitation device was introduced for stroke victims. It involved the patient placing their lower arm into a brace where the robot would then provide support and guidance. While the system used impedance

control to provide safe assistance, the patient was restricted to the table during use.

Motorized Upper Limb Orthotic System (MULOS) was developed in 1997 by Johnson *et al.* [10] to give support in five degrees of freedom for wheelchair users. These degrees of freedom were at the shoulder, the elbow and for pronation/supination of forearm. It provided three different modes; Assistive mode, which amplified muscles and led the hand to a desired position, Continuous Passive Motion, or CPM, where pre-programmed cyclical movements were implemented, and Exercise mode in which resistance training with variable force control was used. There is no information on the progression of this device except that it was discontinued in 1997, possibly due to safety and/or power issues.

2.1.2 Design Issues

Despite the specialised features of these devices, there are still many issues to be resolved with regards to the safety, power, kinematics and control. The fact that these devices were also mounted to tables and wheelchairs restricted the user's mobility and prevented total patient comfort.

Safety of the device is paramount. While safe operation is important to keep the patient from physical harm, a safe perception from the patient's viewpoint is vital for mental health and comfort of the patient. The device must be reliable for all operations and in all environments where materials like water, dust, or grease are present. Simple fitting and removal, known as donning and doffing is also an important feature.

The power of the device is important in determining how effectively it can provide assistance to the patient. All of the rehabilitation devices described above had issues with mass and the accurate automatic compensation for gravity forces and therefore needed to be tethered to the ground via the wheelchair or an external scaffold.

Due to the human arm's ability to orient itself into many different positions, the orthosis must cater for as many degrees of freedom as possible. In order to assist patients in training and rehabilitating any muscle group, the device must have the capability of providing assistance in all degrees of freedom in this case, the seven degrees of freedom shown in the upper limb.

Control is a major issue when it comes to using these assistive technologies. Without an accurate and precise control system, the device may be ineffective or in some cases, dangerous. Real time functioning is also important to allow the smooth operation of the device. The processing power must be adequate in order to input the EMG signals, do the necessary computations and output commands to actuators at a rate that the patient requires.

2.1.3 Muscle Suits

Kobayashi *et al.* [11] describes using a muscle suit to assist upper arm movement. Using pneumatic artificial muscles, the suit aims to provide lightweight physical support for patients. The actuators are sewn into the fabric of the suit which avoids the use of a heavy metal frame. However this does cause some problems including a diminished range of motion which is due to the distance between the actuator and the joint and energy loss. The energy loss occurs due to the slippage and slack of the suit. If the suit is made tighter to avoid these issues, it becomes uncomfortable and difficult to put on for the patient. While there have been some modifications to the design, including the use of a hard external frame, there are still mobility and weight issues affecting the range of movement.

2.1.4 Exoskeletons

There have been many companies which have developed exoskeletons by the encouragement of the medical as well as the military industries. Companies like Raytheon-Sarcos [12] and Cyberdyne [13] have developed wearable robotics suits which assist the user in completing daily activities as well as extraordinary tasks like lifting heavy weights without fatigue.

Raytheon-Sarcos's latest military creation, the Raytheon XOS 2 allows the soldier to lift 77kg, the average weight of a military pack, as if it were only 4.5kg. This will improve the energy consumption for the soldier so that more effort can be put towards other more important tasks. However, there are still issues with the power source as the suit requires a tether to work for a prolonged period. As well as improving the power and life of the battery, other improvements involve lowering the weight and the cost of the device.

Cyberdyne has taken a different approach and focussed on the medical and rehabilitation side of exoskeletons. Their device, the HAL-5 (Hybrid Assistive Limb) uses EMG sensors to determine the intention of the user and motors to assist in the task at hand, for example lifting heavy patients onto a hospital bed.

2.1.5 Powered Upper Limb Orthotics

A recent innovation in upper limb exoskeletons for rehabilitation is the NEUROExos [14, 15, 16], which aims to provide effective kinematic coupling with the anatomical upper arm while implementing a bio-inspired activation scheme.

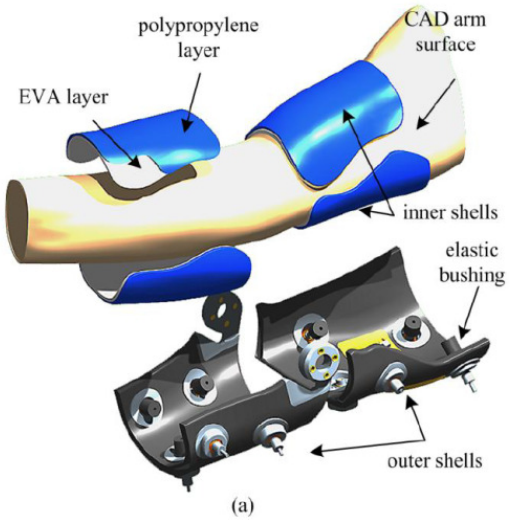

Figure 1: Exploded view of the NEUROExos two shelled design [17]

Permission granted: see Appendix E: IEEE

The design, which couples to the anatomic human arm by the use of two shells, is described in great detail in the study by Vitiello *et al.* [17]. The outer shell, made

from carbon fibre, provides stiffness and strength while supporting the joint and the actuation system. The inner shell, made from a thermo-forming material supports the limb, improves comfort and allows for size adjustments. Both shells are designed to match the shape of the arm to reduce the bulk of the device and are separated by a complex mechanism which is used to provide small adjustments in four degrees of freedom (see Figure 1). This mechanism acts to provide the maximum alignment with the patient to reduce unwanted shear forces which leads to skin irritations and discomfort.

This device achieves its purpose by the use of motor-driven cables to deliver the required torque at the joints. This mechanism is quite heavy and bulky and needs to be attached to the ground via a chair or scaffold of some kind to operate correctly. This means that the patient will be restricted to the one position during the whole rehabilitation process.

2.2 Requirements for Design

In order to design a powered rehabilitation device, the following requirements were developed using the issues listed in the previous section and the study conducted by Tsagarakis and Caldwell [7]:

- Inherent safety and comfort
- Low mass with excellent power/ weight ratio
- Low cost and ease of fabrication
- Functional range of motion

2.2.1 Inherent Safety and Comfort

Due to the direct contact with the patient, the device must be safe and reliable. The patient must also perceive the orthotic as safe in order to maximise their confidence and ‘peace of mind’. Safety controls can be both mechanical and electrical in nature to provide a safe experience for the user. Mechanical stops would include physical barriers at the end of the range of the motion, while the electrical controls would control the speed and the range of movement of the

device using encoders. Due to extended periods of use the orthotic must be comfortable and allow for easy fitting/ removal. In order to cater for patients of different shapes and sizes, the device should be adjustable and adaptable to ensure the comfort of all patients.

Schiele and van der Helm [18] developed an incredibly ergonomic upper limb robotic device. They found that misalignments and oversimplification of anatomical joints led to skin irritation and discomfort. While wearable exoskeleton devices were more robust against these issues, compared to externally mounted robots, additional degrees of freedom should be included in the design to improve the overall adaptability to the body's polycentric joints.

When analysing elbow motion, Schiele and van der Helm suggested the use of two passive degrees of freedom to improve comfort and ergonomics. An adjustable strut length and a hinge at the forearm support (see Figure 2) would allow the orthosis to adjust to the misalignments between anatomical and device joint centres.

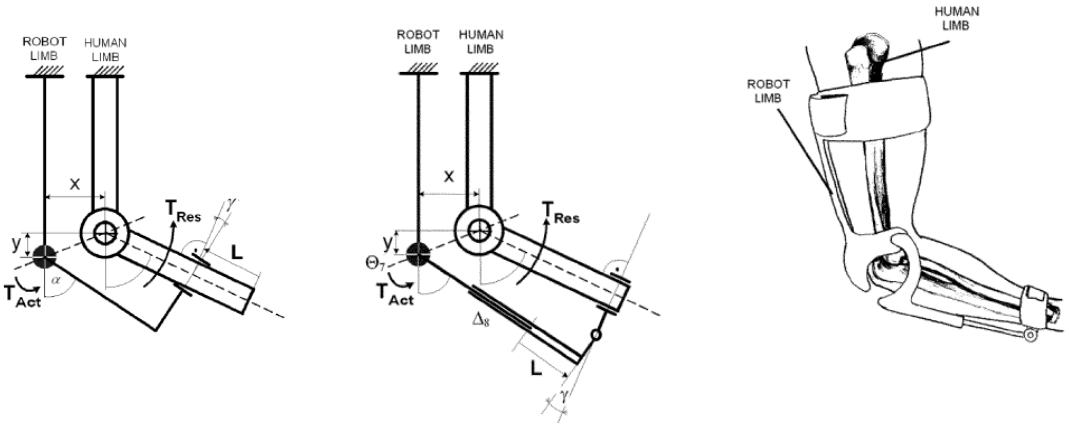

Figure 2: Modifications for elbow orthosis to improve ergonomics [18]

Permission granted: see Appendix E: IEEE

2.2.2 High Power/ Weight Ratio

The biggest contributors to the weight of the device are the mechanical design and the materials used. In order for the orthotic to work effectively in both holding itself up and providing assistance and support to the patient, the mass needs to be kept to a minimum. If the orthotic is too heavy, much of the device's power will go into

lifting itself using gravity compensation measures instead of assisting the patient with movement. While the design can be optimised to increase the power to weight ratio, the type of actuators are important in this requirement.

2.2.3 Low Cost and Ease of Fabrication

A low cost and simple design is important when considering the budget of the project. Although prototypes are inherently costly, through reducing the complexity of the design and striving for low engineering costs and efficient manufacturing the price can be limited. Thought must also go to on-going manufacturing costs in the event that the device goes into production. This means that all machining processes, for example all hole measurements should be consistent throughout the device. Maintenance costs will always be involved in budgeting, and therefore the design should require low to no maintenance during the product life cycle.

2.2.4 Functional Range of Motion

To provide complete assistance the device must match the workspace of a human arm. The workspace of an average human elbow is 5° - 145° but Hsu and Goldberg [19] documented that a range of 30° - 135° is adequate to achieve satisfactory function in all everyday activities. The greater the range of motion, the more difficult it is for the actuator to provide the force needed to assist the patient; this needs to be taken into account.

2.3 Actuator Design

Actuators have varying size, mass, power to weight ratios as well as other properties that must all be considered when designing the orthosis. Motor-driven cables are commonly used in upper arm orthotics but recently pneumatic muscle actuators (pMAs) have been implemented in the medical industry.

Caldwell *et al.* [20] reviewed the major advantages and disadvantages of electric motors, hydraulic and pneumatic actuators that are commonly used to power robotic devices. While electric motors are easy to control in both position and velocity and are relatively cheap and quiet, they are bulky, heavy and have low

power/torque to weight ratios. Hydraulic actuators have higher power to weight ratios but are expensive and noisy. Pneumatic actuators are the cheapest but are difficult to control and are also quite noisy.

Caldwell *et al.* went on to develop the pneumatic muscle actuator, or pMA (see Figure 3). This innovative device is based on an older design known as the McKibben Muscle; it has a high power/ weight ratio, inherent safety while maintaining a low profile. It works by inflating a flexible inner cylinder which is only restricted at either end so that the device can contract and elongate with varying pressure. An outer nylon sheath provides support and protection from over-inflation and ruptures. However, the actuator does require a loud and bulky pressurised air source which may affect patient comfort and confidence in the device.

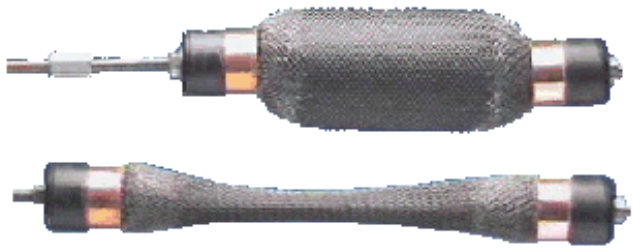

Figure 3: Pneumatic muscle actuator in compression and elongation [21]

Permission granted: see Appendix E: Wikimedia Commons

2.3.1 Shape Memory Alloys

Shape memory alloys, or SMAs, are also finding their way into the industry. These metals are interesting in the way that they can change phase while remaining solid. These phases are known as martensite and austenite. During the martensite phase, the metal can undergo plastic deformation in order to attain different shapes; though when it is heated it changes to the austenite phase which brings it back to its original shape [22].

Shape memory alloys have many advantages including a low profile (allowing them to be easily used in parallel), large power/ weight ratio, simple current control and silent operation. Though they do have a few disadvantages such as low operating

frequencies (which are due to cooling and heating times), hysteresis behaviour and low strain limitations.

Interestingly, these memory materials can be moulded into different shapes depending on what is required for the design. While produced mainly in wire form, some distributors offer a range of memory springs. These springs can be used when a greater force or when a large contraction distance is needed. For the current design, these shape memory springs may be practical as a large contraction is necessary to gain the functional range of motion.

The speed of contraction is limited by the input current while the relaxation speed is limited by cooling rate. Tadesse *et al.* [23] showed three different techniques used to increase the relaxation speed: Forced Air Cooling, Heat Sinking and Liquid Immersion.

Tadesse *et al.* found that forced air cooling could improve the cooling rate up to 75 per cent depending on the level of flow while heat sinking displayed similar results. Liquid immersion, or fluid drenching, produced improvements of up to 87 per cent though the additional friction caused by fluid viscosity may have affected other properties. Though each of these methods showed promising results, power consumption was dramatically increased due to the negative effect of continuous static cooling. If a design is to be as efficient as possible, cooling must only occur when the actuators are not being heated.

Chapter 3: Design Methodology

The following chapter outlines the development stages of the powered upper arm orthosis and the knowledge gained and modifications made to enhance the design to a final prototype.

3.1 Structural Design & Optimisation

3.1.1 Stage One

A simple mechanical design was used for the basis of the orthosis in which two struts are made to rotate about a joint, imitating the anatomical structure of the upper limb. A group of actuators were attached to these struts at different distances in order to assist in elbow flexion and extension. The mounting was kept open as to allow for different actuators including motor-driven cables, pneumatic muscles actuators or shape memory alloys. The top of the device, where the device would attach to the patient's shoulder was also left open for later revisions of strap design.

Figure 4: Rendered CAD model of the basic design for the device

While the device was kept compact in order to avoid obstruction with the patient during movement and reduce orthotic mass, the size reduction was limited by the

mounting of the actuators at larger distances from the pivot to increase the moment arm and therefore the torque that they could apply. The design would be light and cheap to make, but would not be comfortable or supportive for the patient especially due to the fact that it would be attached on only one side of the arm. Due to the fact that this design was simply used as a basis, there was no thought to how the patient's arm would be suspended on this particular design.

3.1.2 Stage Two

A moulded support device was then designed in which a larger area is used to support the patient's arm weight making the device more comfortable. While the internal faces of both upper and lower supports would be moulded for comfort, the external faces would be modified to allow for mounting gravity compensation springs and the actuators. These springs can be used to counter the load of the device while the actuators are left unrestricted to assist motion. Additional holes could be introduced into the design to allow for adjustable mounting in case greater forces are needed from the actuators.

Figure 5: Annotated rough model of second revision of the orthotic design

However the device has the potential to be quite expensive and heavy, depending on materials that are used. A trade-off between strength and weight will need to be taken into account in order to select the most appropriate material, or composition of materials that would be best for the device.

While comfort is a major requirement of the design, other factors such as adaptability and safety should also be taken into consideration. Adaptability would be improved by the use of adjustable straps though the moulded supports would restrict the capabilities of the device to cater for different users. Mechanical stops would also be incorporated into the design to assist any electrical control measures in maintaining patient safety during use.

Optimisation of the actuator placement was achieved using the trigonometric equations described below;

$$\alpha = \tan^{-1}\left(\frac{x+y\cos\theta}{y\sin\theta}\right), \text{ and} \quad (1)$$

$$d = x\sin(90° - \alpha) = x\cos\alpha. \quad (2)$$

Where: x = distance along the upper arm,

y = distance along the forearm,

θ = angle of the elbow,

α =angle of the actuator with the horizontal plane, and

d = moment arm of the actuator about the elbow.

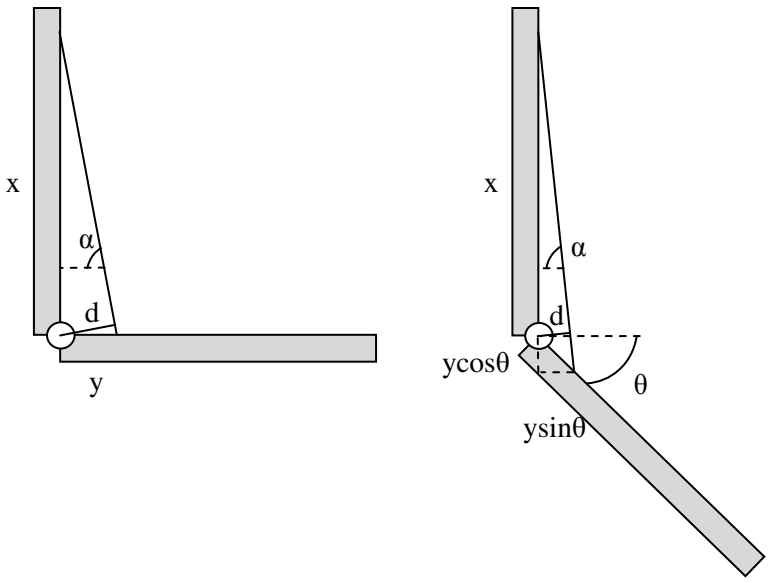

Figure 6: Calculation of the actuator moment arm throughout range of motion

In order to calculate the moment arm, the angle that the actuator makes with the horizontal plane is calculated using the distances of the mountings and the angle of the elbow (see Equation 1). Using geometry rules and similar triangles, the moment arm can then be calculated using this angle and distance of the upper arm mounting from the joint (see Equation 2).

As the forearm moves in relation to the upper arm, the distance that both flexors and extensors are from the axis of rotation changes (see Figure 6). This means that during extension, the flexors need to produce more force and during flexion, the extensors need to produce the greater force.

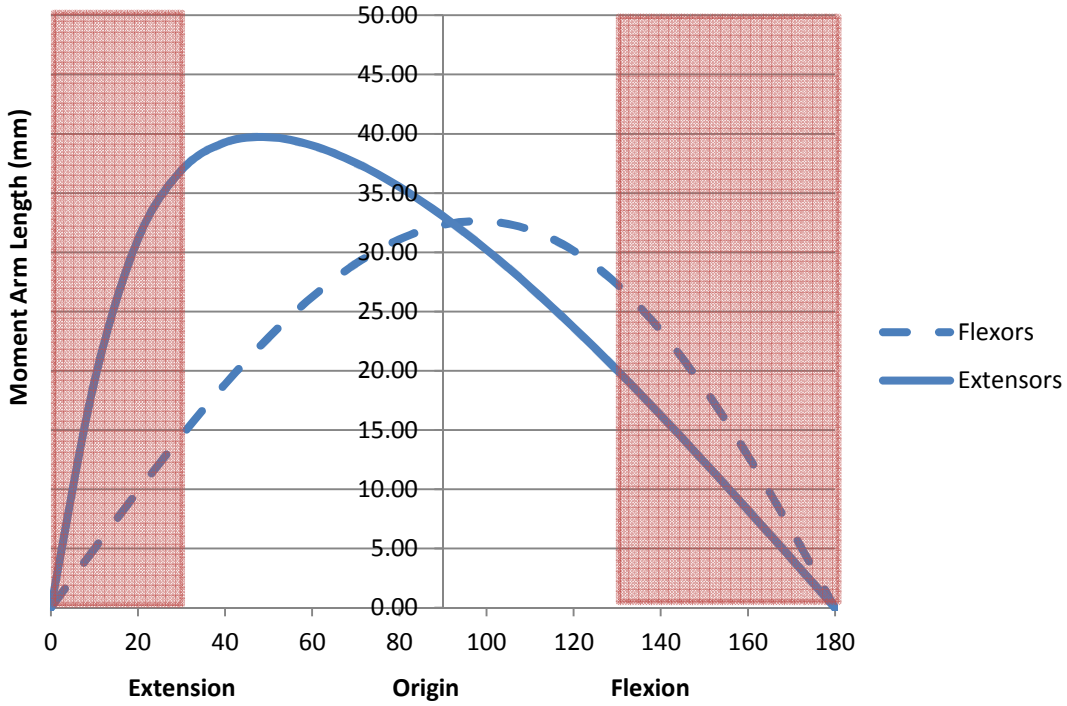

Figure 7: The moment arm length change over functional range of 30° to 130°

As the moment arm decreases, the force supplied by the actuators must increase in order to counter the mass of the arm and orthosis and assist the patient's movement. At approximately 10° flexion, the flexors are at their greatest distance from the axis of rotation and can therefore produce their highest torque at this position (see Figure 7). At approximately 40° extension the extensors can produce their highest torque. Due to the fact that the moment arm is largest at these

positions, the actuators are able to deliver a large amount of force to return the device back to the origin. This is similar to the natural anatomy of the human body where flexors are stronger in flexion and extensors are stronger in extension.

Using the functional elbow range of 30 to 130° taken from Goldberg and Hsu's ATLAS of Orthoses and Assistive Devices [19], the range of the device can be decreased in order to keep the moment arm large enough to achieve reasonable forces. Although, the current design requires a contraction of 19% for the flexors and a contraction of 64% for the extensors, which is quite large for shape memory wires, it may be capable for shape memory springs. To increase the forces, multiple SMAs can also be used in parallel in order to share the load.

3.1.3 Stage Three

Due to the previous design's inability to adapt to different patients, another viable design involving segmenting the supports was evaluated. With the use of smaller supports and Velcro straps, different arm sizes can be accounted for. The device is also adjustable for different limb lengths using a large array of mounting holes. While the device uses additional metal struts, the size reduction in the supports would serve to counter the extra weight from these struts.

Figure 8: Rendered CAD model of the orthotic design with segmented supports

The actuator position can be optimised using the mounting holes and can be moved depending on requirements on the bulkiness of the design and the power needed.

Similarly to the last design, the optimisation of the actuators was conducted in much the same way. Using trigonometry (see Figure 9), the moment arm behaviour during elbow movement was found for both flexors and extensors.

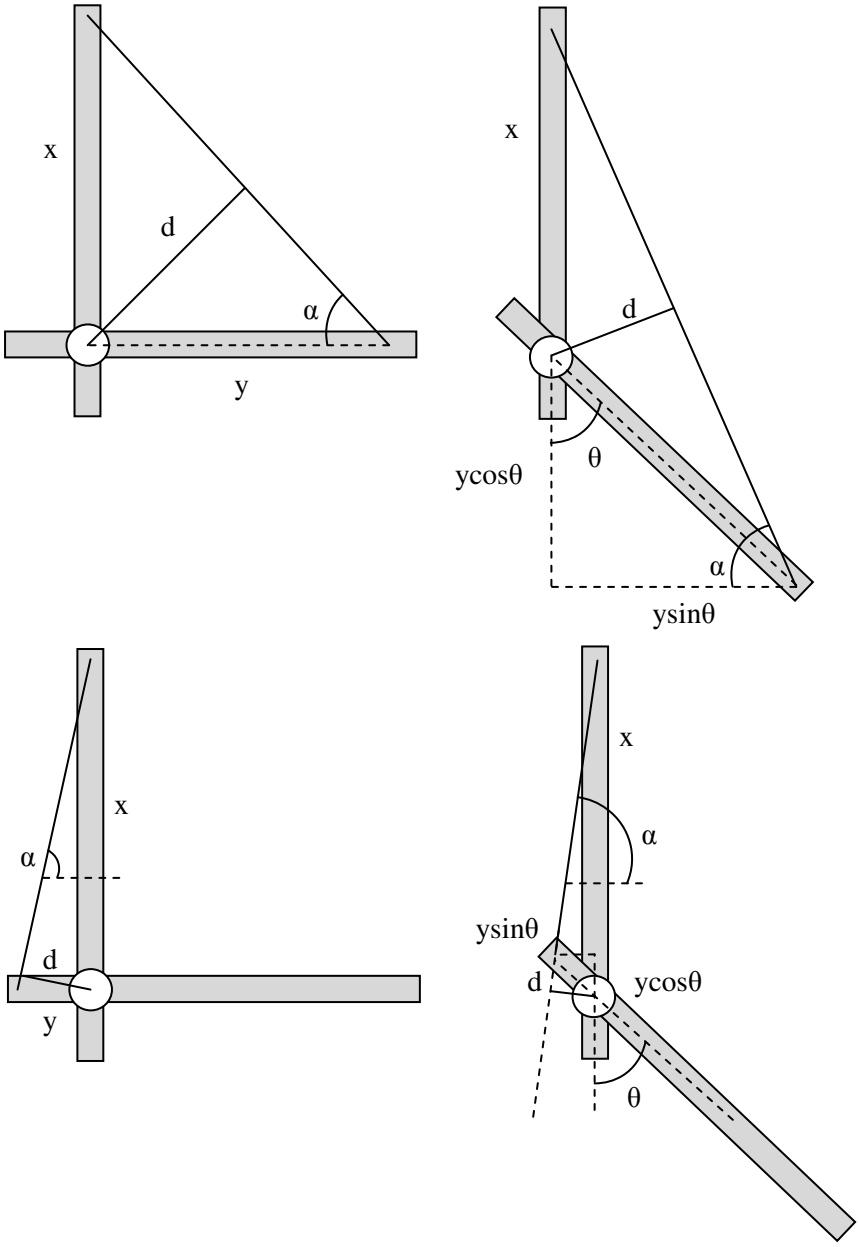

Figure 9: Calculation of the actuator moment arm throughout range of motion

Using this current design, the moment arm length can be seen to change according to elbow angle (see Figure 10).

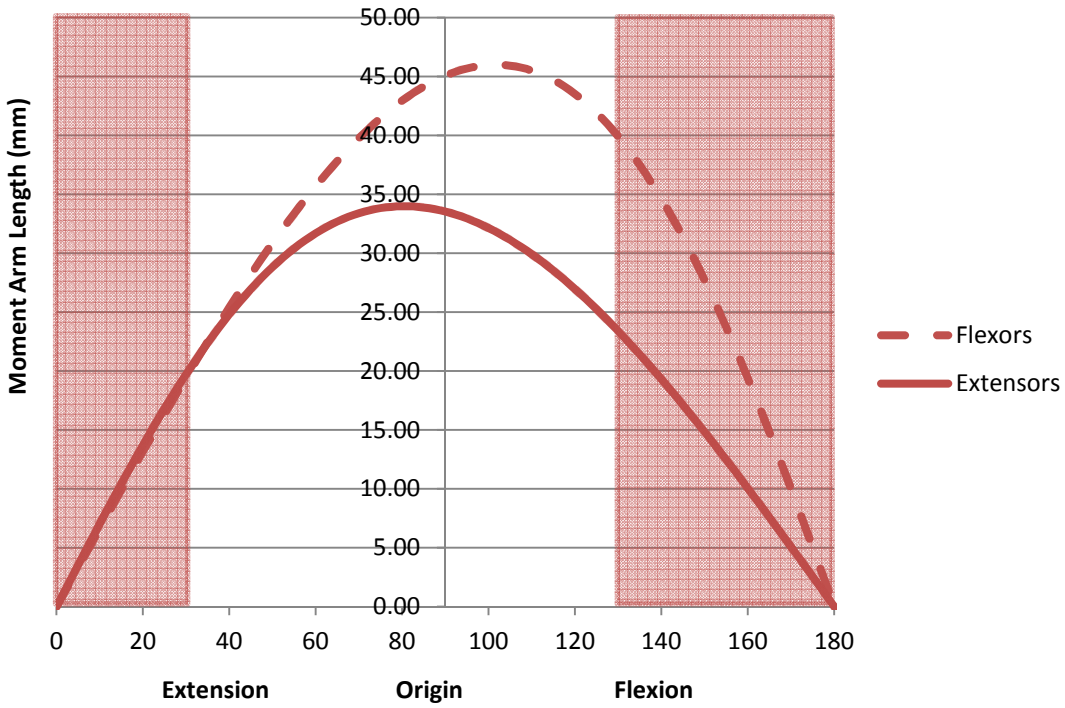

Figure 10: The moment arm length change over functional range of 30° to 130°

The length of the extensor moment arm is roughly even about the origin showing a maximum distance at about 10° extension from the origin. This distance decreases during flexion and higher levels of extension, but due to the fact that gravity is assisting the extensors, the load experienced by these actuators is lower than the actuators assisting flexion.

While these flexor actuators show significantly larger moment arm lengths during flexion, the distance drops rapidly as the device goes into extension. Due to the fact that the moment arm of the actuator in high levels of extension is quite small, springs can be used to assist in returning the patient's arm back to a neutral position.

To ensure the safety of the device, the mechanical design of the struts has been adapted to prevent movement beyond the functional range of motion (see Figure 11). When it reaches 30° extension, the two rotating struts will contact each other preventing any further motion. The same modifications can be used to prevent excessive flexion.

Figure 11: Mechanical stops used to ensure patient safety at maximum extension

Gravity compensation springs were also implemented in the design to assist the flexors in lifting the weight of the arm, though they would work against the extensors. Depending on the strength and size of the spring used, the design of the spring would be modified to allow for no effects during flexion by the use of an enlarged slot at one end of the spring (see Figure 12a).

When the device is in excessive flexion, the mounting slides down the slot in order to disengage the spring. When the device begins to extend, the mounting screw slides back up the slot and then stops at the end to allow the spring to start to extend and provide an assistive force.

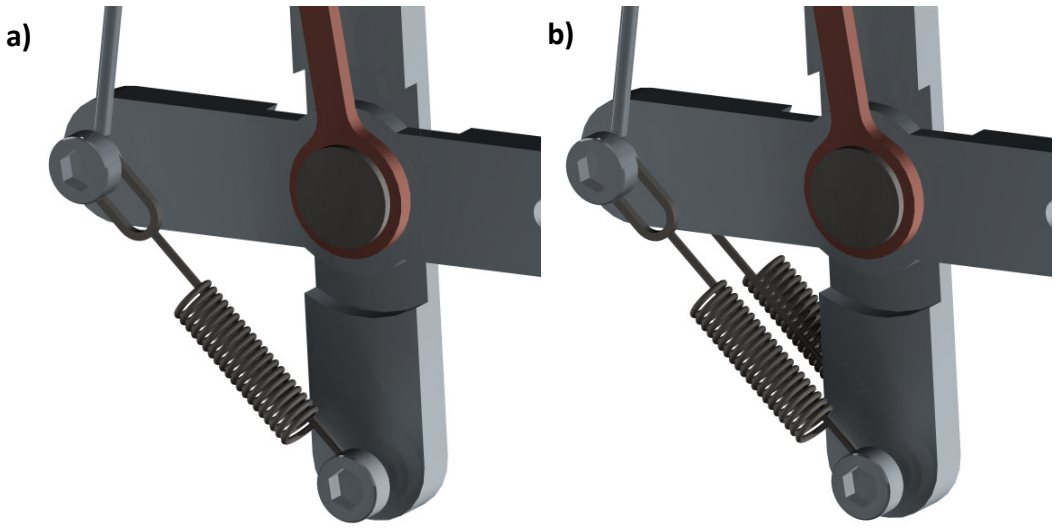

Figure 12: a) Single gravity compensation spring design and **b)** double spring design.

In order to achieve the most suitable spring dimensions, the required force needs to be calculated using mechanical analysis and the mounting positions optimised to find the appropriate free length and maximum extension available on the market.

Spring retailers such as Lee Spring Company [24] have a large range of springs with different specifications. Variations in outer diameter and wire diameter are the main contributors to force output as the company does produce many springs at different lengths. The table below lists several options available from the company.

Table I: Springs Available from Lee Spring

Part Number	Outer Diameter	Wire Diameter	Free Length	Max. Length	Max. Load	Price
LE029C04M	6.35mm	0.736mm	35mm	68mm	19.1N	£1.96
LEM120EB01M	13mm	1.2mm	30mm	58mm	42.2N	£2.20
LEM120CE03S	8.5mm	1.2mm	40mm	66mm	52.3N	£2.52
LEM140ED01M	15mm	1.4mm	35mm	66mm	57N	£2.33
LE 063F 01M	15.88mm	1.6mm	50.8mm	89mm	66.7N	£2.90
LE 069F 01M	15.88mm	1.8mm	50.8mm	81.5mm	84N	£2.90

There is also the option of using two springs on each side of the orthosis instead of a single spring (see Figure 12b). This would provide a greater force but may encroach on the patients elbow reducing comfort and safety. Using stronger springs will also affect the extensors ability to move the arm into extension.

3.1.4 Final Stage

If shape memory alloys are selected for the driving mechanism, modifications need to be made to the design to ensure the actuators can respond to fast movements. Gorbet and Russell [22] developed a dynamic cooling model using a moving heat sink that assisted in cooling only when the shape memory alloy was not being activated. This design showed large improvements in relaxation times without the same negative effects during contraction, keeping power consumption low.

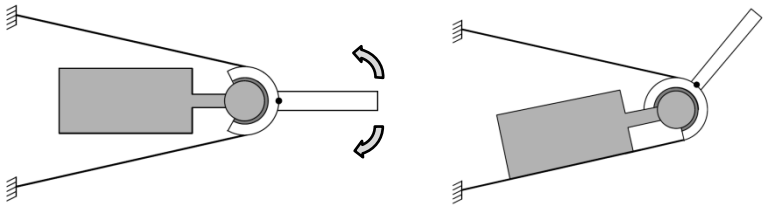

Figure 13: The mechanism designed by Gorbet and Russell in 1995.

Permission granted: see Appendix E: Cambridge University Press

The mechanism (see Figure 13) contains the heat sink which is attached to the joint with the use of a friction clutch. This clutch allows the heat sink to instantaneously move between actuators depending on which is contracting. A similar method has been implemented in the current design for the elbow orthosis.

Additionally, Jain and Goodson [25] stated that due to the low thermal conductivity of shape memory alloys, the active cooling would only be localised to a small segment of the actuator. The remaining wire would remain at high temperatures inhibiting the heat sink from cooling the overall actuator and increasing contraction speed. The design must therefore contact a greater area to provide cooling to as much of the wire as possible.

There may also be issues with the retention of heat inside the heat sink, which would affect the mechanism's ability to cool the wire. Liquid or air cooling may be required to diffuse the heat inside the block. Taking into consideration manufacturing issues, a method that could be used is described below.

The heat sink assembly would be comprised of three different pieces of the same shape. A channel would be cut into one side of the base; the medium would flow into this channel from an external source, circulate through the heat sink, and remove the heat as it returned out of another port (see Figure 14c). A gasket (Figure 14b) would be placed over the base, and a cover (Figure 14a) would secure it in place. The gasket would serve to seal the groove preventing any medium leakage, although greater measures may be required for heavier flow (e.g. an O-ring seal instead of gasket seal). Thermal testing would be required to discover if this assembly is necessary or if a simple block is sufficient to cool the actuator.

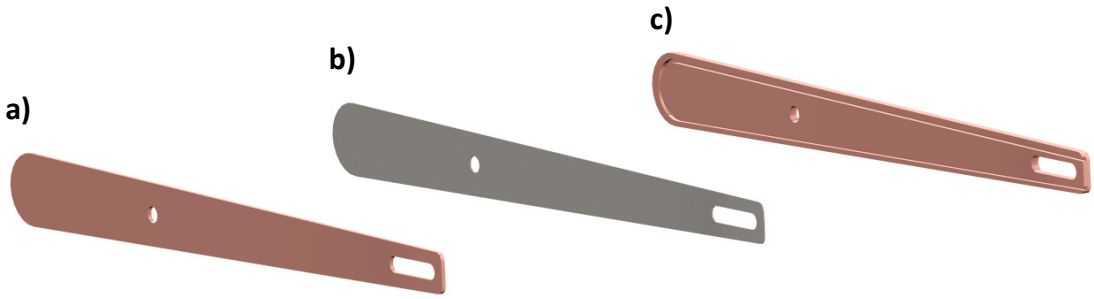

Figure 14: a) Cover, **b)** gasket and **c)** base of the heat sink assembly

With regards to the general wearability of the device, Vitiello *et al.* [16] expressed concerns about designs utilising bar linkages with cuffs for patient support. These designs have been known to encounter issues with comfort, inertia and kinematic compatibility. Appropriate modifications were incorporated into this design to counter these issues.

The main issue relates to the complexity of the elbow joint, where the device's single axis joint is not sufficient in providing comfortable assistance to the patient. As prescribed by Schiele and van der Helm [18], to improve the ergonomics of the device, the bottom support must be designed to have a variable length during use and the support must be able to handle some rotation.

The first of these passive degrees of freedom involves the extension on the bottom strut of the device. This was achieved by segmenting the strut into two different bars and using a sliding slot joint between them. Each slot contains two screws to

counter and transfer the load of the arm to the actuators during use and to maintain alignment. A third set of screws is attached to the first strut and is used to mount an extension spring or elastic band (see Figure 15 and Figure 16). This small mechanism is used to ensure the second bar returns to the initial position to ensure comfort of the patient.

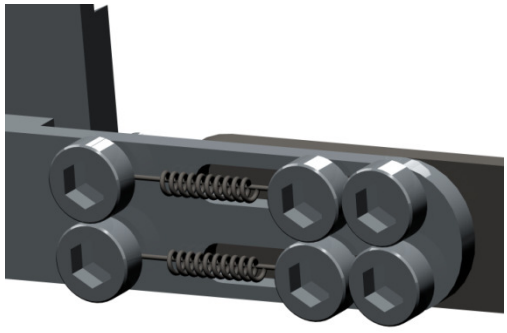

Figure 15: The use of small extension springs for the mechanism.

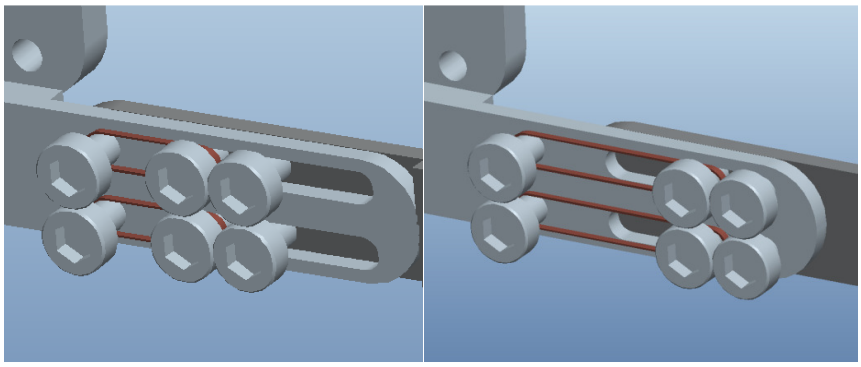

Figure 16: The passive mechanism (using bands) in extension

Due to the prototype nature of the design, the screws were used as pins to slide inside the slot. If the screws were substituted for bearings, any friction issues would be resolved and product life would be extended. This is important to note, for future revisions of the device.

The second degree of freedom requires the strap to allow for low levels of rotation. Velcro straps were used instead of hard supports to assist in this requirement as well as the device's overall patient adaptability. These straps would secure the patient's arm to the device while the hard supports would remain to ensure rigidity of the device and the alignment of the joint.

A model of the final design is shown in Figure 17.

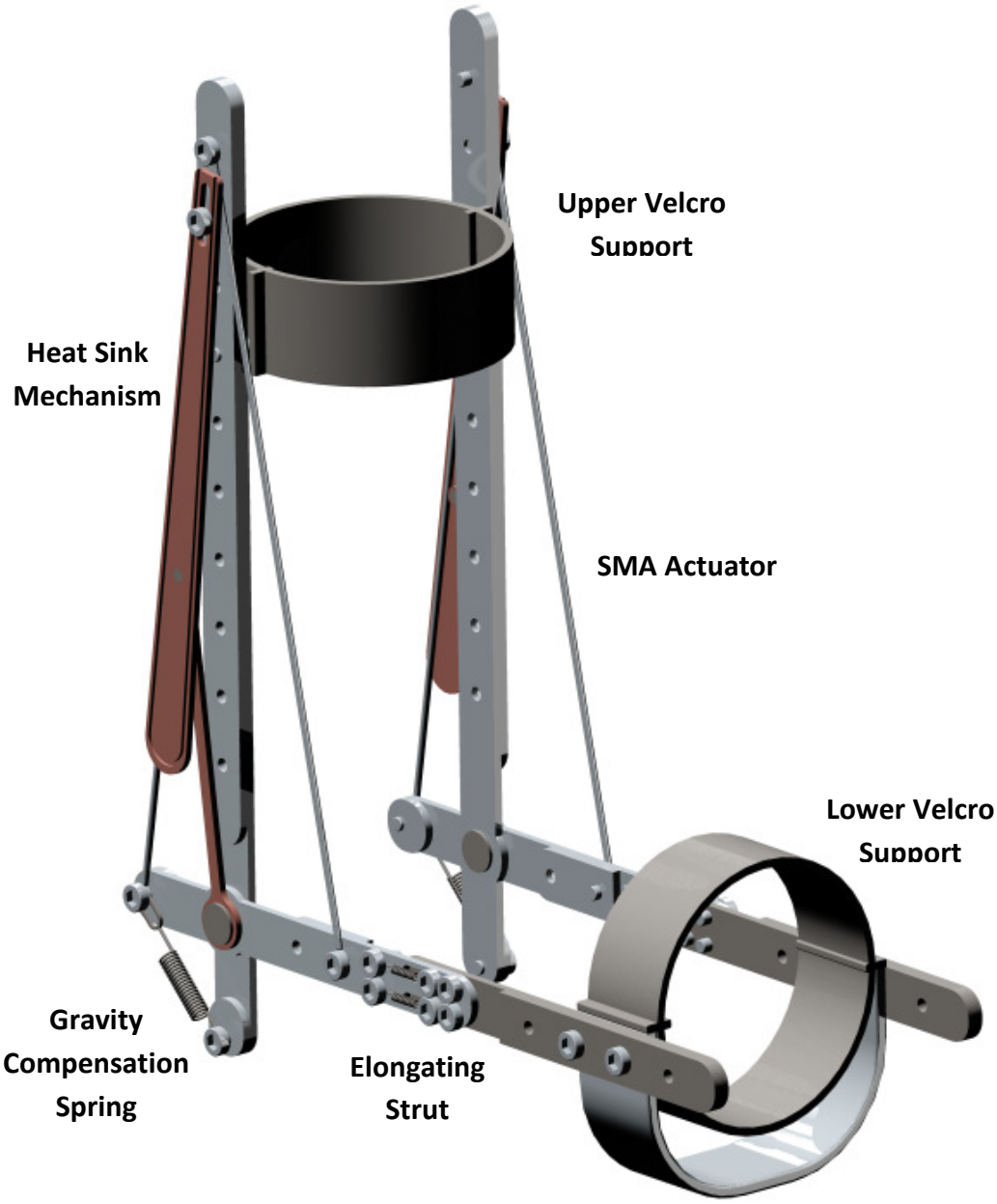

Figure 17: The final design of the device.

Upon consultation with an orthotist from the National Centre of Prosthetics and Orthotics (NCPO) of the University of Strathclyde, Glasgow an issue with the current strap design was raised. The recommendation involved the installation of a sling or cup to hold the elbow in place and improve the force distribution of the lower arm to the device.

3.2 Material Selection

The materials considered for this project were compared in terms of strength, weight, cost and manufacturability using Granta's CES Edupack®.

Due to the fact that the frame makes up majority of the mass of the design, an appropriate material choice is important. The following categories were examined individually:

- Plastics
- Metals
- Composite Fibres

Plastics, including polymers and thermosetting plastics are commonly found in orthotics due to their light weight and low cost. Co-polymer and homo-polymer polypropylene have been used for in the orthotics industry for many years for their established manufacturing processes and their material properties. Silicones are flexible polymers that may be used to provide a comfortable barrier between the patient and the device. This would be achieved by lining the contacting areas of the device with the material.

The strongest material group considered were the metal group where aluminium, steel and titanium were researched. Aluminium is cheap and easily manufactured but has lower strength properties. Mild steel is stronger, but heavier. Titanium exhibits desirable strength and weight but is quite expensive and may not be practical for low-cost large scale production.

Composite fibres are the most modern option and exhibit many desirable properties. Examples such as pre-impregnated carbon composites are strong and light materials, but are mainly used for customised products due to the manufacturing process.

The heat sink must be made of a material that has a large thermal conductivity. Copper has an incredibly high thermal conductivity but is quite heavy and

expensive, while other metals like aluminium have a midrange thermal conductivity but are lighter and cheaper. This is the trade-off that needs to be considered. If fluid cooling is required, the gasket which seals the heat sink assembly should be made from a waterproof material with some flexibility such as neoprene or rubber.

The screws, pins and springs should all be standard materials and sizes in order to improve manufacturing and production costs. Common materials used for these parts are a range of steels, although due to the potentially corrosive environment of this medical device, stainless steel should be considered.

Shape memory alloy actuators come in a range of commercially available products which are all based on a nickel and titanium composite [23]. Two of the most widely distributed SMA wires are Flexinol from Dynalloy Inc., USA and Biometal fiber from Toki Corporation, Japan.

The straps used to secure the patients arms to the device have been designed to be Velcro for the material's inherent application for fastening but also due to its strength, low weight and usability.

Table II: Material Selection Table

Component	Material	Notes
Frame	Metal Plastic Composite Fibre	Dependent on availability and material and manufacturing costs.
Heat Sink	Copper (priority) Aluminium	Dependent on cost and the thermal conductivity needed.
Springs, Screws and Pins	Steel/ Stainless Steel	Standard materials and sizes to reduce costs.
SMA	Nickel-Titanium Composite	
Straps	Velcro	

Each component was updated in the model to display the correct properties taken from assumed materials. This was necessary to gain an accurate model in the simulation software.

3.3 Strap Design

Due to the fact that the device is only assisting in elbow flexion and extension, there needs to be some thought on how the patient will wear the device and where the weight will be distributed. The strap must be light weight, comfortable, easy to don and doff and provide sufficient support.

Cool [26] described the mechanics of upper limb orthoses and the importance of rectifying shoulder subluxation, where the shoulder joint is unstable; commonly seen in patients with brachial plexus injuries and hemiplegia. The subluxation is caused by the weight of the upper and lower limbs pulling the arm out of the already weakened shoulder joint. Therefore, a strap must be utilised which provides a force sufficient to counter these weights as well as providing some resultant force in the shoulder to neutralise any subluxation.

The Wilmer Strap, reviewed by Plettenburg [27, 28] is a possible basis for a strap design which transfers the weight of the arm and the device to the patient's shoulder and chest while effectively eliminating any shoulder subluxation. While the Wilmer shoulder orthosis aims to balance the lower arm in a horizontal position, the current powered design uses actuators to control this position and therefore the only requirement is that it is weight bearing and provides sufficient support to the shoulder joint.

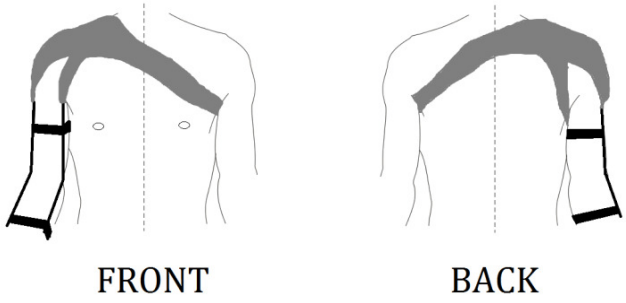

Figure 18: Simple sketch of a possible strap design for the device [29]

A strap that goes directly to the adjacent shoulder may also be used to benefit patients with severe shoulder injuries on the affected arm, reducing pain and improving comfort of the device.

3.4 Completing the Arm

Ultimately, the elbow orthosis will be a part of a larger device which will encompass the shoulder and the wrist. Due to this requirement, considerations were made to the design with respect to how the current device will be assimilated with a shoulder mechanism.

The details of shoulder design will not be covered in this study, but some understanding of this complex system is needed in order to understand how the final product will go together. The shoulder can be separated into three different degrees of freedom: flexion-extension, adduction-abduction and medial-lateral swing. While flexion-extension rotation aims to raise and lower the arm, adduction-abduction rotation allows movement of the arm away from and toward the body medial-laterally. The last rotation, medial-lateral swing, revolves around longitudinal axis of the upper arm.

Figure 19: The final device with shoulder attachment.

A passive mechanism was designed that allowed shoulder movement in each of these rotations. This shoulder mechanism is attached to a large support bracket that serves to maintain rigidity of the overall system as well as combining the two segments together via a set of bolts at the upper arm.

Chapter 4: Motion Analysis

The motion analysis of the device involves static, kinematic and dynamic studies into the forces and related behaviour of the device. To verify the results from these calculations, a simulation was also conducted on MATLAB® Simulink.

4.1 Static Analysis

Statics is the branch of mechanics that studies the forces that are applied on a stationary rigid body. By the use of free body diagrams, the forces and moments, both internal and external, are calculated and balanced. This is necessary in finding the force required from the strap, the gravity compensation springs and to work toward calculating the tension applied to the actuators.

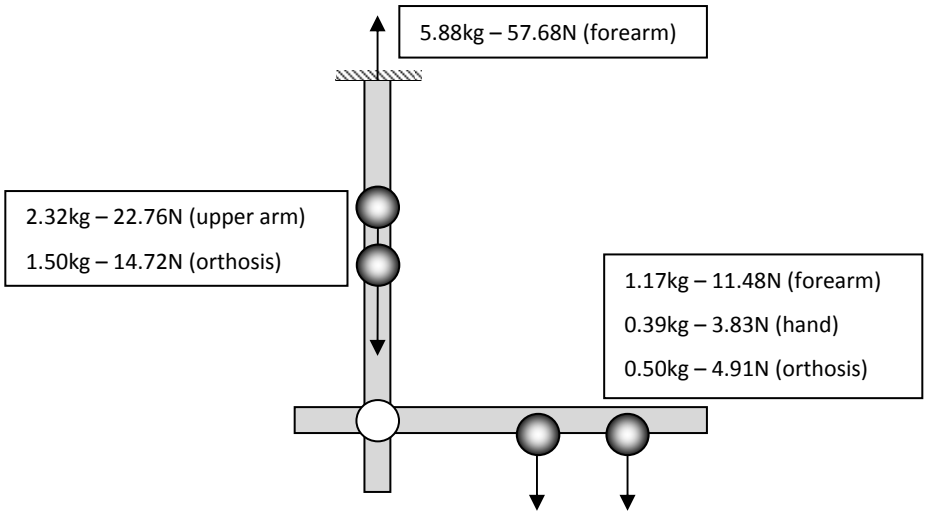

Figure 20: Free Body Diagram of the orthosis

Using the information given from Drillis and Contini [29], the average weight and limb lengths were found using a 1.7m average adult weighing 65kg. The estimated weight for the device was 2kg, with upper and lower sections of the orthosis weighing 1.5kg and 0.5kg respectively (see Figure 20).

The force needed from the strap is easily found using a free body diagram of the system and using the following force balance equation in the vertical direction.

$$\sum F_{vertical} = F_{strap} - F_{arm} - F_{orthosis} = 0 \quad (3)$$

While conducting an analysis on the overall system is important to calculate the forces on the strap, the device can also be separated into its upper and lower segments (see Figure 21). Using this method, the forces that affect each individual segment can be analysed separately. These free body diagrams are essential when calculating the moment around the joint allowing the tension in the springs to be found. Using the limb lengths given from Drillis and Contini and other assumptions regarding the uniformity of each segment (centre of mass being central to each section), the moment was calculated from the lower limb free body diagram.

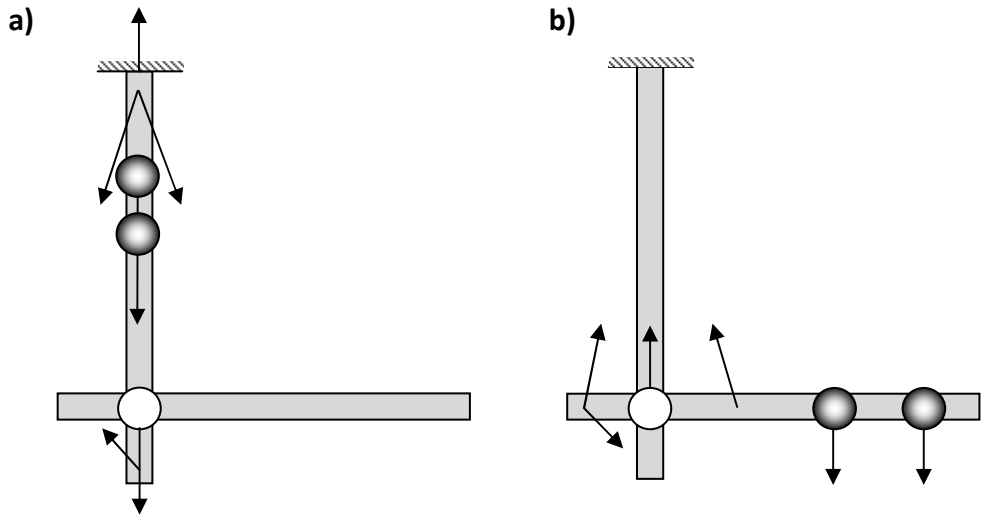

Figure 21: a) Free body diagram of upper limb only and **b)** the lower limb only

The springs were used to counter the static moment around the joint. As the moment arm of the springs is a lot smaller than that of each centre of mass, the force required of them is quite large. The tension in the actuators was left to power the movement of the arm only with the magnitude depending on the speed and acceleration required for the patient. While in reality, these actuators would play some part in countering these weights, the assumption can be made in order to evaluate the spring parameters required easily.

$$\sum M_{lower} = 2 \cdot F_{spring} \cdot d_{spring} - m_{arm} \cdot g \cdot d_{arm} - m_{orth.} \cdot g \cdot d_{orth.} = 0 \qquad (4)$$

The tension in the springs can be calculated using Newton's Law of Inertia where the force applied by the actuators equals the linear and angular inertia of each centre of mass. The following equation is a modified moment balance equation for the flexing of the elbow, where the effects of the extensors are ignored.

$$2 \cdot T_{flexor} \cdot d_{flexor} = m_{arm} \cdot a \cdot d_{arm} + m_{orth.} \cdot a \cdot d_{orth.} + I_{arm} \cdot \alpha + I_{orth.} \cdot \alpha \qquad (5)$$

The symbols, a and α represent acceleration of the centre of mass and angular acceleration of the link respectively.

Using estimates of values given by the literature and derived from the CAD model, the force applied to the spring is approximately 59N. Although this is quite substantial it is within the capabilities of the springs produced by Lee Springs [24].

The maximum tension produced in each memory wire with a 250µm diameter was found in the literature as 9N [31]. Using this value, both of the equations above were used to calculate the maximum angular acceleration of the lower segment. Current estimates put the acceleration as 87.43deg/s^2 in flexion and 55.64deg/s^2 in extension which is more than adequate for rehabilitation training. Therefore the limiting factor of the acceleration of the device would be the inherent cooling period of the shape memory actuators.

The moment around the elbow joint was found to reach a maximum magnitude of 2.84Nm when horizontal. This value includes both the weight of the orthosis and the arm of the patient. This value will be verified by other methods of analysis in the following segments of this chapter.

4.2 Kinematic Analysis

Kinematics is the study of how things move. It is a branch of mechanics which describes the motion of objects without consideration of the forces which cause the motion. Without using kinematics as a basis for analysis, robotic control cannot be achieved.

Forward kinematics describes the position and orientation of a robot's end-effector based on the length of the links and the angles of the joints. Robots can be broken down into two main components, joints and links. A joint represents a pivot (usually controlled via an actuator) while a link represents the connection between these joints. In the case of robotic arms, the joints are the 'elbows' of the device and the links are the upper and lower limbs. The kinematics can be expressed as $T = f(\theta)$ where T is position and orientation of the end-effector and $f(\theta)$ is the equation of motion in terms of angles.

The most commonly used notation for defining links and joints throughout the world of robotics is *Denavit-Hartenberg (D-H) technique* [32] (see Figure 22). It describes the robot motion mathematically and is used to find the forward kinematics of the system. It works by referencing a frame to each link then mapping out each link frame in relation to the preceding link frame. The symbol i is used to number each joint in the series from 1 to *n*, while each joint i connects link i-1 to link i.

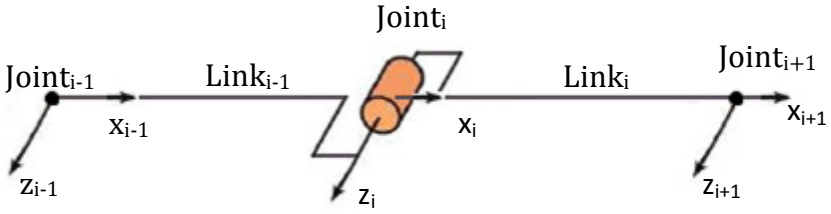

Figure 22: An example schematic diagram of a robotic system

To assign the link frames, the z vector, denoted by z_i is always along the joint axis, so that the joint rotates about that line, and the x vector, represented by x_i is located perpendicular to both z_{i-1} and z_i and orientated from z_{i-1} to z_i. The origin of

the frame is situated at the intersection of both of these vectors while orientation of the frame is chosen so that the angle around z_i is positive.

The D-H technique goes on to obtain the four necessary parameters required for describing the relationship between each link. These parameters are α_{i-1}, a_{i-1}, d_i and θ_i, where;

α_{i-1} is the *link angle*; the twist angle between two axes of z_{i-1} and z_i along x_{i-1}.

a_{i-1} is the l*ink length*; the link distance between two axes of z_{i-1} and z_i along x_{i-1}.

d_i is the *link offset*; the offset distance between two axes of x_{i-1} and x_i along z_{i-1}.

θ_i is the *link twist*; the joint angle between two axes of x_{i-1} and x_i along z_{i-1}.

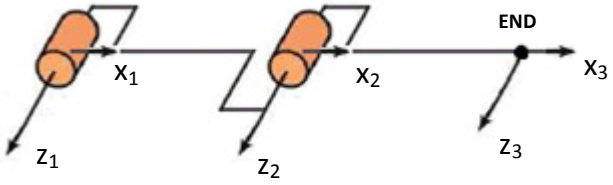

Figure 23: Schematic Diagram for the Elbow Orthosis

Once these parameters are found, they are placed in a D-H table (see Table II) so that the transformation matrix can be calculated. This matrix aims to describe the relationship between each of the link frames of the orthotic device.

Table III: D-H Table for Elbow Orthosis

i	α_{i-1}	a_{i-1} (mm)	d_i (mm)	θ_i
1	0°	0	0	θ_1*
2	0°	L_1	0	θ_2
3	0°	L_2	0	0

*where the shoulder is assumed to be constrained to flexion/extension only.

From this information, the transformations between each frame can be found using the following equation;

$$ {}^{i-1}T_i = \begin{bmatrix} R_i & P_i \\ 0 & 1 \end{bmatrix} = \begin{bmatrix} \cos\theta_i & -\sin\theta_i & 0 & a_{i-1} \\ \sin\theta_i \cdot \cos\alpha_{i-1} & \cos\theta_i \cdot \cos\alpha_{i-1} & -\sin\alpha_{i-1} & -d_i \cdot \sin\alpha_{i-1} \\ \sin\theta_i \cdot \sin\alpha_{i-1} & \cos\theta_i \cdot \sin\alpha_{i-1} & \cos\alpha_{i-1} & d_i \cdot \cos\alpha_{i-1} \\ 0 & 0 & 0 & 1 \end{bmatrix} \quad (6) $$

Where R_i and P_i are the rotation and translation matrices.

The final objective of forward kinematics is to obtain a matrix which shows the position and orientation of the end-effector in relation to ground, or in this case, the part of the device that is attached to the shoulder. Now that the transformation from each frame is known, the following equation can be used to find the final position matrix;

$$ {}^{BASE}T_{EE} = {}^{BASE}T_1 \cdot {}^{1}T_2 \cdot {}^{2}T_3 . \quad (7) $$

The base frame can be placed at the centre of the shoulder so that there is no translation or rotation from the base frame to the first frame.

$$ {}^{BASE}T_{EE} = \begin{bmatrix} \cos\theta_1 & -\sin\theta_1 & 0 & 0 \\ sin\theta_1 & cos\theta_1 & 0 & 0 \\ 0 & 0 & 1 & 0 \\ 0 & 0 & 0 & 1 \end{bmatrix} \begin{bmatrix} \cos\theta_2 & -\sin\theta_2 & 0 & L_1 \\ sin\theta_2 & cos\theta_2 & 0 & 0 \\ 0 & 0 & 1 & 0 \\ 0 & 0 & 0 & 1 \end{bmatrix} \begin{bmatrix} 1 & 0 & 0 & L_2 \\ 0 & 1 & 0 & 0 \\ 0 & 0 & 1 & 0 \\ 0 & 0 & 0 & 1 \end{bmatrix} $$

$$ {}^{BASE}T_{EE} = \begin{bmatrix} \cos(\theta_1+\theta_2) & -\sin(\theta_1+\theta_2) & 0 & L_1\cos\theta_1 + L_2\cos(\theta_1+\theta_2) \\ \sin(\theta_1+\theta_2) & \cos(\theta_1+\theta_2) & 0 & L_1\sin\theta_1 + L_2\sin(\theta_1+\theta_2) \\ 0 & 0 & 1 & 0 \\ 0 & 0 & 0 & 1 \end{bmatrix} $$

All matrix calculations can be seen in Appendix A while the MATLAB® code used to verify the results can be seen in first code segment in Appendix B.

If the shoulder is restricted with zero rotation, the position and orientation are described by the transformation matrix shown below;

$$ {}^{BASE}T_{EE} = \begin{bmatrix} \cos(\theta_2) & -\sin(\theta_2) & 0 & L_1 + L_2\cos(\theta_2) \\ \sin(\theta_2) & \cos(\theta_2) & 0 & L_2\sin(\theta_2) \\ 0 & 0 & 1 & 0 \\ 0 & 0 & 0 & 1 \end{bmatrix}. $$

Due to the ergonomic design of the device, L_2will be vary as the arm extends. Although a relationship must be found between L_2 and θ_2, before the exact position of the end effector can be found.

Another branch of kinematics is called *Inverse Kinematics*. Rather than the calculation of the position and orientation of a robot's end-effector based on all of the joint angles as it is in forward kinematics, inverse kinematics asks what motions are necessary to allow a robot's end-effector to reach a desired position. Due to the simplicity of the system at hand, the inverse kinematics can be calculated using geometry and trigonometry although inverse kinematics does get dramatically more complex with more degrees of freedom.

$$x = L_1 \sin\theta_1 + L_2 \sin\theta_2$$

$$y = L_1 \cos\theta_1 + L_2 \cos\theta_2$$

The inverse kinematics is necessary for control when the position is known but the level of actuation is required. Control theory will be expanded in Chapter 5.

4.3 Dynamics

Once the forward kinematics is found, the next step is to calculate the dynamics of the system. Unlike kinematics, dynamics takes all of the forces of the system into account when describing the motion of the system. This allows for a more accurate model to be found.

There are many ways of finding the dynamics mathematically. Methods such as the *Lagrangian Formulation* [33] use conservation of momentum and energy to calculate the dynamic equation while *Newton-Euler Dynamics* [34] method is used for more complicated systems and uses Newton's laws of physics.

The Newton-Euler method does not need to calculate kinetic or potential energy of links but simply the velocity and acceleration using equations that will work in any situation. Due to this fact, the Newton-Euler Iterative Method was chosen over the Lagrangian Method. With the potential for modifications to the current system and

additional degrees of freedom, the iterative calculations can be easily modified in order to gain an accurate model regardless of mechanical complexity.

Before the dynamics can be found the moment of inertia of each link must be calculated as unlike kinematic analysis, links cannot be assumed as massless. The moment of inertia is an objects resistance to rotational changes and is located on a certain axis called the *inertia tensor*.

$$I_C = \begin{bmatrix} I_{XX} & I_{XY} & I_{XZ} \\ I_{YX} & I_{YY} & I_{YZ} \\ I_{ZX} & I_{ZY} & I_{ZZ} \end{bmatrix} \tag{8}$$

Mass Moments of Inertia

$$I_{XX} = \iiint_V (y^2 + z^2)\rho \, dV, \qquad I_{YY} = \iiint_V (x^2 + z^2)\rho \, dV, \text{ and} \qquad I_{ZZ} = \iiint_V (x^2 + y^2)\rho \, dV. \tag{9}$$

Mass Products of Inertia

$$I_{XY} = I_{YX} = -\iiint_V xy\rho \, dV, \qquad I_{XZ} = I_{ZX} = -\iiint_V xz\rho \, dV, \text{ and} \qquad I_{YZ} = I_{ZY} = -\iiint_V yz\rho \, dV. \tag{10}$$

The calculations for the inertia can be seen in the MATLAB® code in Appendix B.

The value I_{XX} denotes the moment of inertia when the object is rotated around the x-axis; I_{YY} denotes the moment of inertia when the object is rotated around the y-axis, and so on. The products of inertia are the contributions from other axes during this rotation and when all of these values are zero, the rotation is said to be around the *principal axes* of the body. At this point, the moments of inertia are known as the principal moments of inertia.

The process of finding the dynamic equation using the Newton-Euler method is broken up into four steps, which are quite iterative in nature allowing easier calculations using the computer programming program, MATLAB®.

Step 1 - Prepare Quantities

The first step requires that all necessary initial constraints be found. The movement of the base or the external forces applied to the end effectors are examples of constraints that need to be taken into account.

Centre of mass	${}^{i}P_{Ci}$
Inertia tensor at the mass centre	I_{Ci}
External force/ torque	${}^{EE}f_{EE}$ & ${}^{EE}n_{EE}$
Motion of the base	${}^{base}\omega_{base}$ & ${}^{base}\dot{\omega}_{base}$ & ${}^{base}\ddot{O}_{base}$

where ω is the angular velocity, $\dot{\omega}$ is the angular acceleration, $\ddot{O}$ is the linear acceleration and ${}_{EE}$ denotes the end-effector. For this project:

$${}^{base}\omega_{base} = {}^{base}\dot{\omega}_{base} = {}^{EE}f_{EE} \;\&\; {}^{EE}n_{EE} = 0 \; and \; {}^{base}\ddot{O}_{base} = \begin{bmatrix} 0 \\ -g \\ 0 \end{bmatrix}$$

Step 2 - Outward Iterations

Outward iterations work from the base to the end-effector, finding the velocities and accelerations of each link using information about the last, and relating it all back to the base. This allows for an accurate model of the movements according to the base, disregarding forces and only taking into consideration angles and transformations from one link frame to the next. The equations used to find each value are given below;

$${}^{i+1}\omega_{i+1} = {}^{i}R_{i+1} \cdot {}^{i}\omega_i + \dot{\theta}_{i+1} \cdot {}^{i+1}z_{i+1}, \tag{11}$$

$${}^{i+1}\dot{\omega}_{i+1} = {}^{i}R_{i+1} \cdot {}^{i}\dot{\omega}_i + ({}^{i}R_{i+1} \cdot {}^{i}\omega_i) \times (\dot{\theta}_{i+1} \cdot {}^{i+1}z_{i+1}) + \ddot{\theta}_{i+1} \cdot {}^{i+1}z_{i+1}, \tag{12}$$

$${}^{i+1}\ddot{O}_{i+1} = {}^{i}R_{i+1} \cdot ({}^{i}\ddot{O}_i + {}^{i}\dot{\omega}_i \times {}^{i}O_i + {}^{i}\omega_i \times ({}^{i}\omega_i \times {}^{i}O_i)), \tag{13}$$

$${}^{i+1}\ddot{O}_{C_{i+1}} = {}^{i+1}\dot{\omega}_{i+1} \times {}^{i+1}O_{C_{i+1}} + {}^{i+1}\omega_{i+1} \times \left({}^{i+1}\omega_{i+1} \times {}^{i+1}O_{C_{i+1}}\right) + {}^{i+1}\ddot{O}_{i+1}, \tag{14}$$

$${}^{i+1}F_{i+1} = m_{i+1} \cdot {}^{i+1}\ddot{O}_{C_{i+1}}, \text{ and} \tag{15}$$

$${}^{i+1}N_{i+1} = I_{C_{i+1}} \cdot {}^{i+1}\dot{\omega}_{i+1} + {}^{i+1}\omega_{i+1} \times (I_{C_{i+1}} \cdot {}^{i+1}\omega_{i+1}). \tag{16}$$

Where ${}^{i+1}z_{i+1} = \begin{bmatrix} 0 \\ 0 \\ 1 \end{bmatrix}$ and O is linear displacement.

Step 3 - Inward Iterations

Inward iterations work back to the base from the end-effector, finding the forces and torques on each of the joints. This stage is where the forces/ torques on the motors are taken into account to gain a more accurate dynamical equation of motion. The equations used to find these values are;

$$^{i}f_i = {}^{i}F_i + {}^{i}R_{i+1} \cdot {}^{i+1}f_{i+1}, \tag{17}$$

$$^{i}n_i = {}^{i}N_i + {}^{i}R_{i+1} \cdot {}^{i+1}n_{i+1} + {}^{i}O_{C_i} \times {}^{i}F_i + {}^{i}O_{i+1} \times ({}^{i}R_{i+1} \cdot {}^{i+1}f_{i+1}), \text{ and} \tag{18}$$

$$\tau_i = {}^{i}n_i^T \cdot {}^{i}z_i. \tag{19}$$

The total torque only takes into account joint torques due to the exclusive use of rotational actuators over prismatic.

Step 4 - Dynamics Equation

The final stage requires the torque to be broken up into components so that it can be easily analysed. The generalized format is shown below;

$$\tau = M(\theta)\ddot{\theta} + V\left(\theta, \dot{\theta}\right) + G(\theta) + F(\theta, \dot{\theta}). \tag{20}$$

Where the each components is as follows:

$M(\theta)\ddot{\theta}$ is the mass matrix,

$V\left(\theta, \dot{\theta}\right)$ is the centrifugal and coriolis term,

$G(\theta)$ is the gravity term, and

$F\left(\theta, \dot{\theta}\right)$ is the friction term, though friction was assumed to be negligible for this project.

The value for torque profile of the elbow joint gained by the simulation was as follows;

$$\tau = -0.0015\dot{\theta}_2^2 + 0.00162\ddot{\theta}_2 - 0.158\cos(\theta_2) + 0.147\sin(\theta_2) + 5.03 \cdot 10^{-8} p\ddot{\theta} - 0.0147$$

Using the following values of angular velocity ($\dot{\theta}$) as 5.7°/s, angular acceleration ($\ddot{\theta}$) as 2.8°/s^2, and density as 2800 kg/m^3, the torque profile was plotted while varying the elbow angle (see Figure 24).

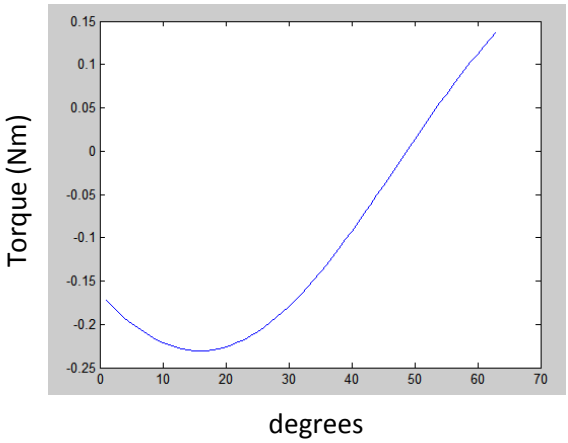

Figure 24: Dynamic analysis of the elbow joint torque

4.4 Simulation

MATLAB® Simulink was used to simulate the device. This simulation software allows the verification of several analysis techniques including forward kinematic, inverse kinematic and dynamics. Initially, a block diagram for a simplified device was created (see Figure 25) in order to test the general kinematics of the design.

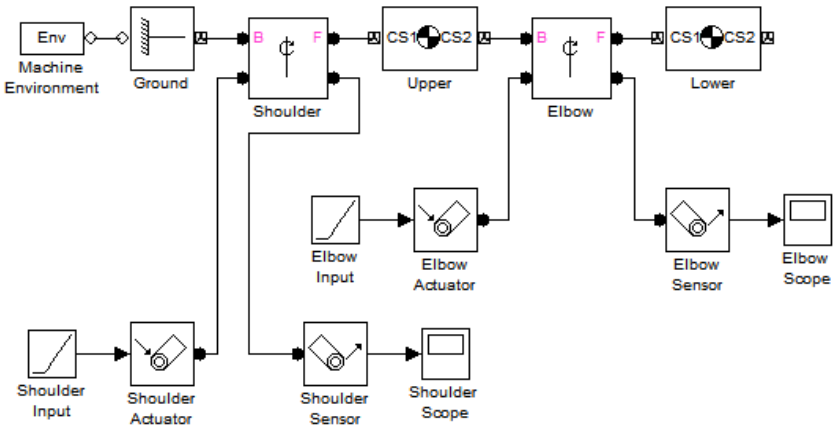

Figure 25: Schematic block diagram of the simplified device

The ground frame was connected to the upper limb with a revolute joint acting as the shoulder which was then connected to the lower limb with another revolute joint for the elbow. For this experiment, the shoulder joint was constrained and fixed into position to limit any rotation in an attempt to imitate the patients shoulder during pure elbow rehabilitation. A joint sensor was used to record the torque at the shoulder during the test, displaying the results on a scope.

The elbow joint was also controlled using a joint actuator, though this joint was controlled with displacement control, where the angle of the rotation is changed via the input source. The torque at the elbow was also recorded in a similar fashion to the shoulder. While this was a simplified model, the simulation gave a good introduction into the use of Simulink and gave an approximate estimation of the torque behaviour likely to be generated in each joint during real testing.

Using the SimMechanics plug-in with Pro|ENGINEER®, the complete model was transferred into a MATLAB® file in order to perform the simulation. This method automatically defines the bodies and joints of the system using the information given by the CAD program (see Figure 26).

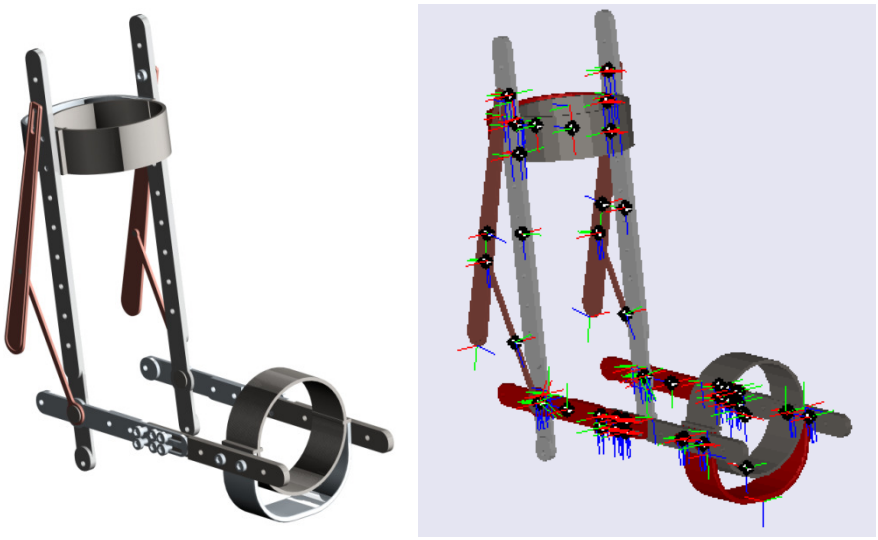

Figure 26: Converting the model for simulation analysis using SimMechanics

The SimMechanics Link process can be found in Appendix C while the created schematic block diagram can be seen in Appendix D.

The simulation was designed to rotate the arm down at 4.5°/s for 10 seconds with a spring dampener implementing at the passive linear elongation segment of the lower strut (see Figure 27).

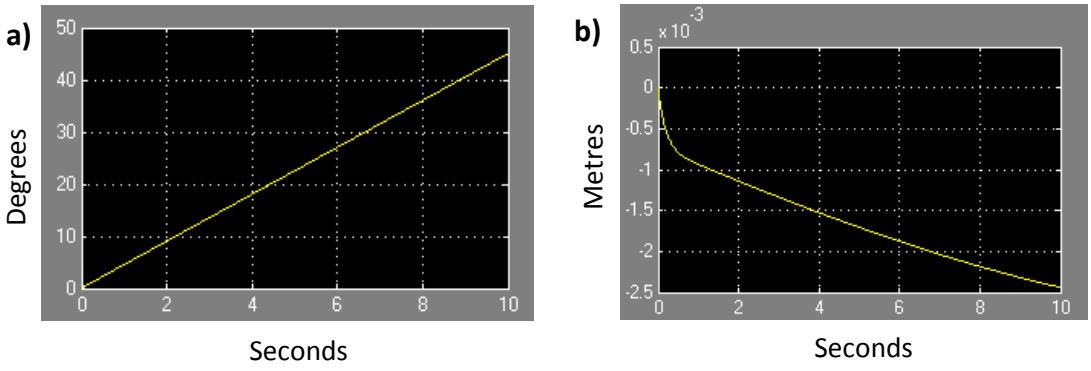

Figure 27: a) Elbow angle during simulation and **b)** linear displacement of strut

The torques at the base show zero moment around the vertical axis (see Figure 28a blue) while the moment about the forward facing axis showed an offset due to the fact that the base was taken from one strut instead of the centre of both struts (Figure 28a pink).

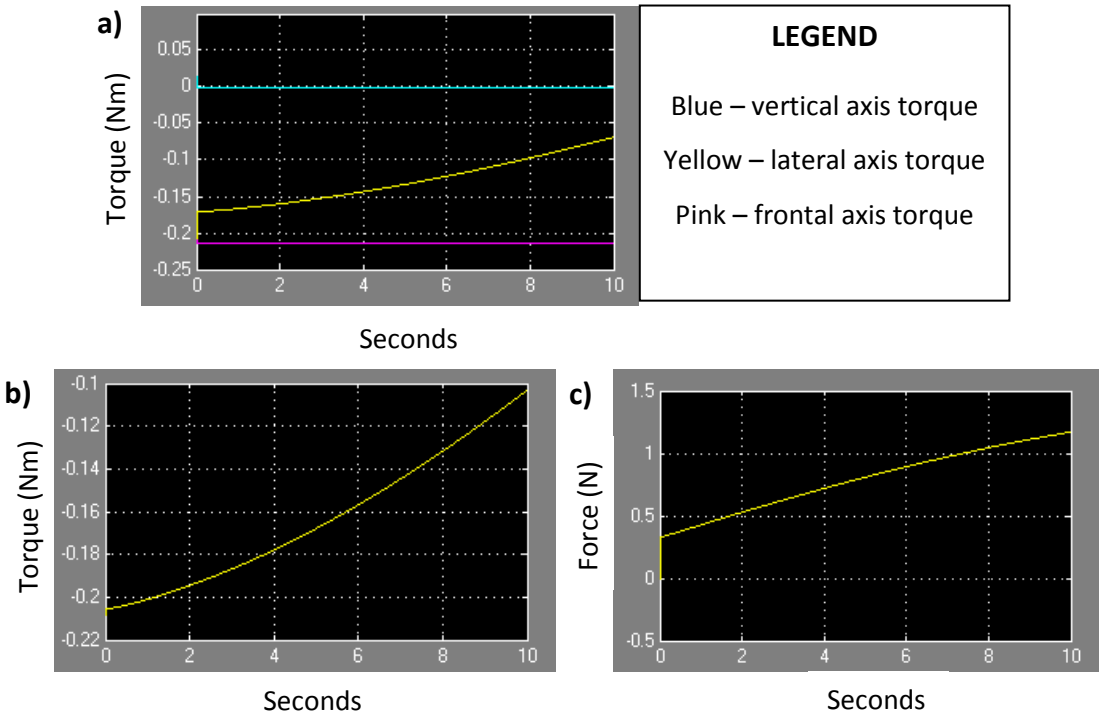

Figure 28: a) Torques around base, **b)** elbow and the **c)** prismatic joint force

The rotation in the medial-lateral axis (Figure 28a yellow) showed similar behaviour to the torque around the elbow (Figure 28b).As expected the torque around the elbow reaching a maximum at 90° flexion and decreases with flexion and extension on either side of horizontal. The force on the springs at the prismatic joint in the lower strut was also examined (Figure 28c).

The simulation results show large similarities in the elbow joint torque with the dynamics analysis especially in the maximum torque where both methods reach a value of just above -0.2Nm. This is interesting to note as the dynamics method, estimated the mass and inertia of the device. It is important to note that both methods ignored the weight of the arm in the device.

In order to simulate the device with the weight of the lower arm, a sphere composed of iron was modelled inside the lower Velcro strap. Using the density given by the CAD software of $6.94 \cdot 10^{-6}$kg/m^3 and the volume of a sphere equation given below (see Equation 21), a mass of 1.47kg was used as a substitute for the weight of the forearm and hand.

$$V = \frac{4}{3}\pi r^3 \tag{21}$$

Similarly to the previous test, the SimMechanics Link was used to convert the model into the simulation environment (see Figure 29).

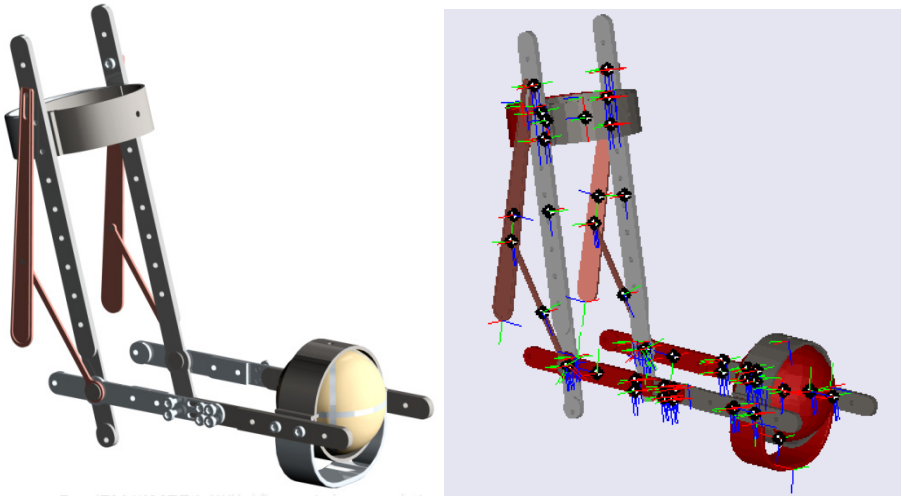

Figure 29: Converting the model with mass using SimMechanics

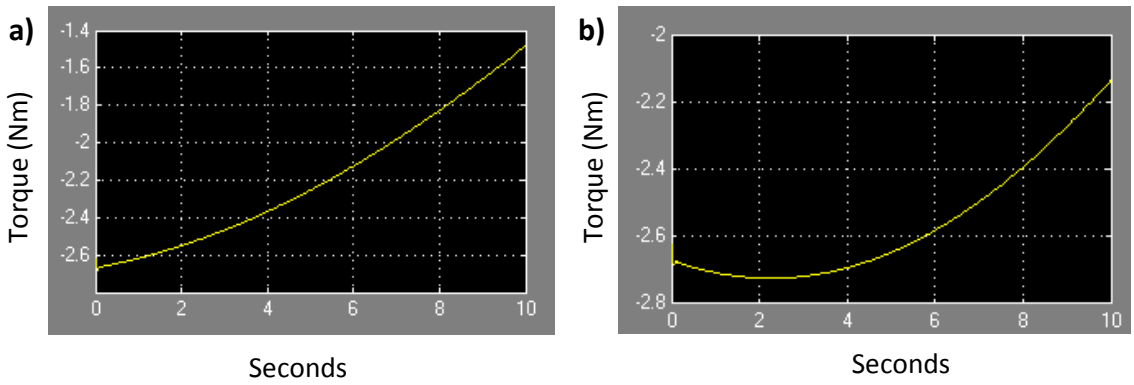

Figure 30: Torques around elbow in **a)** extension and **b)** flexion

The torque around the elbow compares to the values achieved using statics in the first segment of this chapter. The simulation shows that a maximum of approximately -2.72Nm whereas the calculations gave -2.84Nm. This may be due to estimations in weight as well as the additional of a prismatic joint in the lower strut.

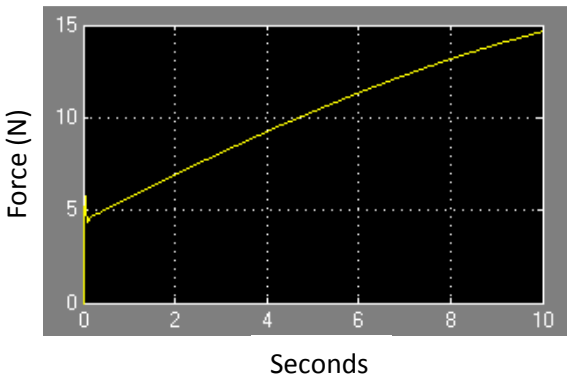

Figure 31: Force in the spring at the prismatic joint

Due to the additional weight of the arm, the springs at the prismatic joint are now under a greater load. With a maximum of approximately 15N, appropriate springs will need to be implemented to allow the strut to return to the original position.

Chapter 5: Conclusions

The mechanical design of the device has been optimised in terms of power/ weight ratio, range of movement, ergonomics and safety. The cost and complexity of the design has also been kept to a minimum.

The power to weight ratio has been the main concern of the project, with majority of the effort going into actuator placement and spring design. The mechanical analysis confirmed that the novel shape memory alloy actuators were strong enough to provide adequate motion to the patient. The contraction/ extension properties of SMA springs would cater for the range of motion required while speed would be highly dependent on the heat sink and the dissipation of heat from the actuators. The necessary spring parameters are met by springs available from manufacturers.

Ergonomics has been considered with the use of Velcro straps and elongating struts. The elongating struts allow for linear movement to account for the complexity of the anatomical elbow joint, while the Velcro straps allow for patient adaptability. Safety measures will be implemented in the control of the device, probably with appropriate current limiters and temperature regulation, although grooves in the struts of the design provide mechanical stops to prevent overextension and excessive flexion.

The complexity of the device was regulated by the use of good manufacturing processes with consistent screw dimensions and limited part complexity. Although some grooves were necessary in the heat sink and the struts which may require the use of a CNC machine. Cost is directly related to this complexity of design as well as the prices for components.

Until a working prototype is fabricated and tested, the only source of analysis are the calculations and the computer simulation which both indicate that the design is both feasible and effective. Once fabrication does occur, further modifications are possible with the use of the multiple mounting holes in the struts.

5.1 Future Recommendations

5.1.1 Control

The next step of the project involves controlling the system. Due to the complicated behaviour of shape memory alloys, including strain hysteresis and a phase transition dependant on temperature and stress, non-linear control approaches are necessary. Control will utilise the mechanics described in the previous chapter as well as closed loop feedback, possibly impedance-based, to determine the angle of the joint, though controlling the physical contraction of the actuator will be incredibly complex due to its thermo-mechanical properties.

Seldon *et al.* [35] discussed the issues with attempts in controlling the entire SMA and described a method of segmenting the wire and controlling each part individually. This Segmented Binary Control technique was able to impose discrete positioning in the wire despite outside influences and showed considerable benefit over other control approaches, particular in preventing cases where sudden changes in load cause unwanted displacement.

5.1.2 Psychological Advancements

Barker *et al.* [36, 37] saw improvement in stroke patients with severe and chronic paresis when performing task-oriented training that is both intensive and repetitive. Using their SMART Arm device, consisting of a simple linear track in which the user would slide their arm, the patient would use visual feedback on muscle strength and limb position to actively participate in their own rehabilitation. The training produced clinically significant results for patients who had suffered from severe strokes in terms of reduced impairment and increased activity. This technique may be a useful feature in the future revisions of powered orthosis.

5.1.3 EMG Sensor Design and Placement

With regards to the sensing technology used to pick up muscle signals, there are several options as to how the electrodes can be placed on the body during use. The following three methods were examined:

- Adhesive
- Bendable Supports
- Clothing (wristband/ sleeve/shirt)

While adhesives are cheap and commonly used in the industry, they can only be used once, require prior knowledge for reliably positioning and are difficult to self-administer. Due to these reasons, adhesives were marked as inappropriate past the initial testing stages of the device.

Bendable supports would be connected to the frame of the device and would allow the patient to position the sensor onto the arm and then remove it once the rehabilitation session is complete. With this there may be issues with maintaining adequate contact during use as the sensor would only be resting on the skin. The patient may also have difficulty in finding the position on the arm that allows the sensor to gain the best results.

The clothing option does have many advantages but may be quite expensive. The EMG sensors would be fitting in the correct positions on the inside of an elastic band or sleeve in which the patient dons before use. Once the device is placed on the arm, the sensors can be plugged into a port on the device to connect the sleeve to the device.

While single-use Ag/AgCl sensors may not be as appropriate to use, alternatives such as reusable dry electromyography sensors are available. These devices produce unchanged signal quality for long periods, are ideally integrated into textiles to determine correct positioning and satisfactory connections and have a high wearing comfort without mechanical or biomechanical stress on the dermal tissue.

Hoffmann and Ruff [38] and Linz *et al.* [39] both found that surface EMG sensors and non-contact sensors had comparable signal quality properties while non-contact sensors tended to last longer due to the fact that no electrolyte gel was used. They found that the sensors worked incredibly well when integrated into tight fitting clothing, giving good results even after being washed in 60°C water.

Figure 32: An example of a shirt that could be used for EMG placement [40]

Taelman *et al.* [41] described the perfect textile as having good elasticity and flexibility to allow stretch and a tight fit, insensitivity to electric charging and favourable moisture and heat regulating properties. Materials like Lycra and other similar materials display these properties and would be a perfect candidate for this type of research (see Figure 32).

5.1.4 Brain Computer Interface

Using a direct interface between the human brain and a computer may improve the control of the rehabilitation device without the need for muscle innervation at all [42]. For patients with severe neural injuries, muscles may not have the required signal output to register on EMG sensors. Using non-invasive Brain Computer Interface techniques such as an EEG electrode cap placed over the user's scalp, has many advantages over invasive electrode implants necessary in the past.

Though research is still being developed in brain pattern recognition, or brain mapping, there are still many issues with the amount of information available from these methods. While advancements in cursor control have been made [43], the user is not directing the cursor directly but activating completely different parts of

the brain in order to gain control. For example, to turn right, the user focuses completely on motion with the right hand, while turning left is achieved by focussing entirely on left hand movements.

With further developments and advancements in brain mapping techniques and improvements in the understanding of the way the brain works [44], this technology may be applicable to this project in the future. This modification would make the device more accessible to patients with more severe neural injuries and may even introduce rehabilitation to patients who find other methods ineffective.

References

[1] World Heart Foundation (2012), Stroke | World Heart Foundation [Accessed online: June 2013]
Available at: http://www.world-heart-federation.org/cardiovascular-health/stroke/

[2] National Stroke Association (2012), Paralysis [Accessed online: June 2013]
Available at: http://www.stroke.org/site/PageServer?pagename=hemiparesis

[3] G. Kwakkel, B.J. Kollen, J. van der Grond and A.J. Prevo (2003), 'Probability of Regaining Dexterity in the Flaccid Upper Limb: Impact of Severity of Paresis and Time Since Onset in Acute Stroke', *Stroke*, Volume 34, pp. 2181-2186.

[4] N. Bayona, J. Bitensky, K. Salter and R. Teasell (2005), 'The Role of Task-Specific Training in Rehabilitation Therapies', *Topics in Stroke Rehabilitation,* Volume 12, Number 3, pp. 58-65

[5] S. Tyson and R. Kent (2011), 'The Effect of Upper Limb Orthotics After Stroke: A Systematic Review', *Neurorehabilitation,* Volume 28, pp. 29-36

[6] G. Kwakkel, B.J. Kollen and H. Krebs (2007), 'Effect of Robot-Assisted Therapy on Upper Limb Recovery After Stroke: A Systematic Review', *Neurorehabiliation and Neural Repair,* Volume 22, Number 2, pp. 111-121

[7] N. Tsagarakis and D. Caldwell (2003), 'Development and Control of a Soft-Actuated Exoskeleton for Use in Physiotherapy and Training', *Autonomous Robots*, Volume 15, Number 1, pp. 21-33

[8] M.A. Alexander, M.R. Nelson and A. Shah (1992), 'Orthotics, Adapted Seating and Assistive Devices', *Pediatric Rehabilitation*, 2nd Edition, pp. 186-187

[9] N. Benjuya and S. Kenney (1990), 'Hybrid Arm Orthosis', *Journal of Prosthetics and* Orthotics, Volume 2, Number 2, pp. 155-163

[10] G. Johnson, D. Carus, G. Parrini, S. Scattareggia Marchese and R. Valeggi (2001), 'The Design of a Five-Degree-Of-Freedom Powered Orthosis for the Upper Limb', *Proceedings of the Institution of Mechanical Engineers*, Volume 215, Part H, pp. 275-284

[11] H. Kobayashi and K. Hiramatsu (2006), 'Development of a Muscle Suit for the Upper Limb – Proposal of Posture Control Methods', *Intelligent Robots and Systems*, 2006 IEEE/RSJ International Conference (ICIRS), October, Beijing, China, pp. 1056-1061

[12] G. Mone (2008), 'Building the Real Iron Man', Popular Science [Accessed online: June 2013]
Available at: http://www.popsci.com/scitech/article/2008-04/building-real-iron-man

[13] Cyberdyne Inc. (2013), 'Robot Suit HAL® | What's "HAL" (Hybrid Assistive Limb®)?' [Accessed online: June 2013]
Available at: http://www.cyberdyne.jp/english/robotsuithal/index.html

[14] E. Cattin, S. Roccella, N. Vitiello, F. Vecchi and M. Carrozza (2008), 'NEUROExos Elbow Module: A New Exoskeleton for Elbow Rehabilitation', *Gerontechnology,* Volume 7, Number 2, pp. 86

[15] T. Lenzi, N. Vitiello, S.M.M. De Rossi, S. Roccella, F. Vecchi and M. Carrozza (2011), 'NEUROExos: A Variable Impedance Powered Elbow Exoskeleton', *IEEE International Conference on Robotics and Automation,* pp. 1419-1426

[16] T. Lenzi, S.M.M. De Rossi, N. Vitiello and M. Carrozza (2012), 'Intention-Based EMG Control for Powered Exoskeletons', *IEEE Transactions on Biomedical Engineering,* Volume 59, Number 9, pp. 2180-2190

[17] N. Vitiello, T. Lenzi, S. Roccella, S.M.M. De Rossi, E. Cattin, F. Giovacchini, F. Vecchi and M. Carrozza (2011), 'NEUROExos: A Powered Elbow Exoskeleton for Physical Rehabilitation', *IEEE International Conference on Robotics & Automation,* pp. 1419-1426

[18] A. Schiele and F. van der Helm (2006), 'Kinematic Design to Improve Ergonomics in Human Machine Interaction', *IEEE Transactions on Neural Systems and Rehabilitation Engineering,* Volume 14, Number 4, pp. 456-469

[19] J. Hsu and B. Goldberg (1997), 'ATLAS of Orthoses and Assistive Devices', *American Academy of Orthopaedic Surgeons*, 3rd Edition, Chapter 5 & 9, pp. 115-124 & pp. 195-208

[20] D. Caldwell, G. Medrano-Cerda and M. Goodwin (1995), 'Control of Pneumatic Muscle Actuators', *IEEE Control Systems*, pp. 40- 48

[21] Rocketmagnet (2007), 'GIF animation of Shadow Air Muscle contracting', *Shadow Robot Company,* [Accessed online: June 2013]
Available at: http://en.wikipedia.org/wiki/File:Sam_animation-real-muscle.gif

[22] R. Gorbet and R. Russell (1995), 'A Novel Differential Shape Memory Alloy Actuator for Position Control', *Robotica*, Volume 13, pp. 423-430

[23] Y. Tadesse, N. Thayer and S. Priya (2010), 'Tailoring the Response Time of Shape Memory Alloy Wires through Active Cooling and Pre-stress', *Journal of Intelligent Material Systems and Structures*, Volume 21, Number 1, pp. 19-40

[24] Lee Spring Company (2013), 'Extension Spring' [Accessed online: July 2013]
Available at: http://www.leespring.com/uk_browse_catalog.asp?springType=E

[25] A. Jain and K. Goodson (2008), 'Measurement of the Thermal Conductivity and Heat Capacity of Freestanding Shape Memory Thin Films using the 3ω Method', *Journal of Heat Transfer*, Volume 130, pp. 102402.1-102402-7

[26] J.C. Cool (1989), 'Biomechanics of Orthoses for the Subluxed Shoulder', *Prosthetics and Orthotics International,* Volume 13, pp. 90-96

[27] D.H. Plettenburg (2000), 'Biomechanics of Upper Limb Orthoses' [Accessed online: July 2013]
Available at: http://www.ispo.nl/upload/file/Plettenburg%20artikel.pdf

[28] D.H. Plettenburg (1998), 'Basic Requirements for Upper Extremity Prostheses: The Wilmer Approach', *Proceedings of the 20th Annual International Conference of the IEEE Engineering in Medicine and Biology Society,* Volume 20, Number 5, pp. 2276-2281

[29] Image adapted from Division of Nursing (2013), 'Cardiology Teaching Package', *The University of Nottingham* [Accessed online: July 2013]
Available at: bit.ly/164hIUy

[30] R. Drillis and R. Contini (1966), 'Body Segment Parameters: A Survey of Measurement Techniques', *Technical Report from School of Engineering and Science*, New York University

[31] R.G. Gilbertson (1993), 'Muscle Wires Project Book', *Mondo-Tronics,* 3rd Rev Edition, Part One: Motorless Motion! pp. 14

[32] J. Denavit and R.S. Hartenberg (1995), 'A Kinematics Notation for Lower-pair Mechanisms based on Matrices," *Journal of Applied Mechanics*, Volume 22, Number 2, pp. 215-221

[33] D. Morin (2008), 'Introduction to Classical Mechanics: With Problems and Solutions', *Cambridge University Press; 1st Edition,* Chapter 6: The Langrangian Method, pp. 165-201

[34] M. Ardema (2005), 'Newton-Euler Dynamics', *Springer Science + Business Media*, Chapter 7: Angular Momentum and Inertia Matrix, pp. 165-186

[35] B. Selden, K. Cho and H. Asada (2004), 'Segmented Binary Control of Shape Memory Alloy Actuator Systems using the Peltier Effect', Proceedings of the IEEE International Conference on *Robotics & Automation*, New Orleans, USA, pp. 4931-4936

[36] R. Barker, S. Brauer and R. Carson (2008), 'Training of Reaching in Stroke Survivors with Severe and Chronic Upper Limb Paresis Using a Novel Non-robotic Device: A Randomised Clinical Trial', *Stroke*, Volume 39, pp. 1800-1807

[37] R. Barker, S. Brauer and R. Carson (2009), 'Training-induced Changes in the Pattern of Triceps to Biceps Activation During Reaching Tasks After Chronic and Severe Stroke', *Experimental Brain Research,* Volume 196, Issue 4, pp. 483-496

[38] K.P. Hoffmann and R. Ruff (2007), 'Flexible Dry Surface-Electrodes for ECD Long-term Monitoring', *Proceedings of the 29th Annual International Conference of the IEEE EMBS*, August, Lyon, France, pp. 5379-5342

[39] T. Linz, L. Gourmelon and G. Langereis (2007), 'Contactless EMG Sensors Embroidered onto Textile', *4th International Workshop on Wearable and Implantable Body Sensor Networks*, pp. 29-34

[40] Image from Wiggle Ltd. (2013), 'Under Armour ColdGear Base Map 1.5 Crew Neck Base Layer' [Accessed online: July 2013]
Available at: http://bit.ly/144Tcnh

[41] J.Taelman, T. Adriaensen, C. van der Horst, T. Linz and A. Spaepen (2007), 'Textile Integrated Contactless EMG Sensing for Stress Analysis', *Engineering in Medicine and Biology Society, Proceedings of the 29th Annual International Conference of the IEEE EMBS*, August, Lyon, France, pp. 3966-3636

[42] R. Megalingam, M. Venkata, A. Gupta T. Dutt (2012), 'EEG Acquisition Device for a Thought Controlled Robotic Arm', *International Journal of Applied Engineering Research,* Volume 7, Number 11

[43] Y. Li, C. Wang, H. Zhang and C. Guan (2008), 'An EEG-based BCI System for 2D Cursor Control, *IEEE International Joint Conference on Neural Networks*, IJCNN 2008. (IEEE World Congress on Computational Intelligence).

[44] N. Petersen, H. Pyndt and J. Nielsen (2003), 'Investigating Human Motor Control by Transcranial Magnetic Stimulation', *Experimental Brain Research*, Volume 152, pp. 1-16

Appendices

Appendix A – Kinematics Matrix Calculations

$$^{BASE}T_{END} = {}^{BASE}T_1 \cdot {}^1T_2 \cdot {}^2T_3$$

$$^{BASE}T_{END} = \begin{bmatrix} \cos\theta_1 & -\sin\theta_1 & 0 & 0 \\ sin\theta_1 & cos\theta_1 & 0 & 0 \\ 0 & 0 & 1 & 0 \\ 0 & 0 & 0 & 1 \end{bmatrix} \begin{bmatrix} \cos\theta_2 & -\sin\theta_2 & 0 & L_1 \\ sin\theta_2 & cos\theta_2 & 0 & 0 \\ 0 & 0 & 1 & 0 \\ 0 & 0 & 0 & 1 \end{bmatrix} \begin{bmatrix} 1 & 0 & 0 & L_2 \\ 0 & 1 & 0 & 0 \\ 0 & 0 & 1 & 0 \\ 0 & 0 & 0 & 1 \end{bmatrix}$$

$$^{BASE}T_{END} = \begin{bmatrix} \cos\theta_1 \cdot \cos\theta_2 - \sin\theta_1 \cdot \sin\theta_2 & -\cos\theta_1 \cdot \sin\theta_2 - \sin\theta_1 \cdot \cos\theta_2 & 0 & L_1\cos\theta_1 \\ \sin\theta_1 \cdot \cos\theta_2 + \cos\theta_1 \cdot \sin\theta_2 & -\sin\theta_1 \cdot \sin\theta_2 + \cos\theta_1 \cdot \cos\theta_2 & 0 & L_1\sin\theta_1 \\ 0 & 0 & 1 & 0 \\ 0 & 0 & 0 & 1 \end{bmatrix} \begin{bmatrix} 1 & 0 & 0 & L_2 \\ 0 & 1 & 0 & 0 \\ 0 & 0 & 1 & 0 \\ 0 & 0 & 0 & 1 \end{bmatrix}$$

$$= \begin{bmatrix} \cos\theta_1 \cdot \cos\theta_2 - \sin\theta_1 \cdot \sin\theta_2 & -\cos\theta_1 \cdot \sin\theta_2 - \sin\theta_1 \cdot \cos\theta_2 & 0 & L_1\cos\theta_1 + L_2(\cos\theta_1 \cdot \cos\theta_2 - \sin\theta_1 \cdot \sin\theta_2) \\ \sin\theta_1 \cdot \cos\theta_2 + \cos\theta_1 \cdot \sin\theta_2 & -\sin\theta_1 \cdot \sin\theta_2 + \cos\theta_1 \cdot \cos\theta_2 & 0 & L_1\sin\theta_1 + L_2(\sin\theta_1 \cdot \cos\theta_2 + \cos\theta_1 \cdot \sin\theta_2) \\ 0 & 0 & 1 & 0 \\ 0 & 0 & 0 & 1 \end{bmatrix}$$

Using the following trigonometric identities:

$$\sin(\theta_1 \pm \theta_2) = \sin\theta_1 \cdot \cos\theta_2 \pm \cos\theta_1 \cdot \sin\theta_2$$

$$\cos(\theta_1 \pm \theta_2) = \cos\theta_1 \cdot \cos\theta_2 \mp \sin\theta_1 \cdot \sin\theta_2$$

$$^{BASE}T_{END} = \begin{bmatrix} \cos(\theta_1+\theta_2) & -\sin(\theta_1+\theta_2) & 0 & L_1\cos\theta_1 + L_2\cos(\theta_1+\theta_2) \\ \sin(\theta_1+\theta_2) & \cos(\theta_1+\theta_2) & 0 & L_1\sin\theta_1 + L_2\sin(\theta_1+\theta_2) \\ 0 & 0 & 1 & 0 \\ 0 & 0 & 0 & 1 \end{bmatrix}$$

Appendix B – Dynamics MATLAB® Code

```
function [x,y,z]=Elbow_Orthosis(theta1, theta2, theta3, theta4,
theta5, theta1dot, theta2dot, theta3dot, theta4dot, theta5dot,
theta1dodot, theta2dodot, theta3dodot, theta4dodot, theta5dodot)
%% DYNAMICS OF ELBOW ORTHOSIS
%% Stefan Di Donato - 201278079
%% Forward Kinematics
% Defining Variables for the System
syms L1 L2
syms theta1 theta2 theta3 theta4 theta5
theta1=0;
L1=0.1425;
L2=0.1;

% DH Table for Elbow Orthosis **MODIFY FOR DIFFERENT SYSTEM**
DH = [0 0 0 theta1; 0 L1 0 theta2; 0 L2 0 0; 0 0 0 0; 0 0 0 0; 0 0 0
0; 0 0 0 0];

% Transformation Matrices
TM = sym(zeros(4,4,7));

% Assigning Frames
for i = 1:7; % counter
 TM(:,:,i)=[cos(DH(i,4)) -sin(DH(i,4)) 0 DH(i,2);
sin(DH(i,4))*cos(DH(i,1)) cos(DH(i,4))*cos(DH(i,1)) -sin(DH(i,1)) -
sin(DH(i,1))*DH(i,3); sin(DH(i,4))*sin(DH(i,1))
cos(DH(i,4))*sin(DH(i,1)) cos(DH(i,1)) cos(DH(i,1))*DH(i,3); 0 0 0
1];
end

% Final Kinematics Equation
TMelbow =
TM(:,:,1)*TM(:,:,2)*TM(:,:,3)*TM(:,:,4)*TM(:,:,5)*TM(:,:,6);

disp(simplify(TMelbow))

%% Newton Euler Iterative Method
%% Declaration of all Variables **MODIFY FOR DIFFERENT SYSTEM**
 theta1dot=0;
 syms theta2dot;
 %theta2dot = 0.1;
 theta3dot = 0;
 theta4dot = 0;
 theta5dot = 0;

 theta1dodot=0;
 syms theta2dodot;
 %theta2dodot = 0.05;
 theta3dodot = 0;
 theta4dodot = 0;
 theta5dodot = 0;

% Joint Angular Velocity
A = [0;theta1dot;theta2dot;theta3dot;theta4dot;theta5dot; 0];

% Joint Angular Acceleration
```

```
B = [0;theta1dodot;theta2dodot;theta3dodot;theta4dodot;theta5dodot;
0];

% Linear Acceleration of the Centre of Mass
Ac = sym(zeros(3,1,7));

% Force at Mass Centre
Fc = sym(zeros(3,1,7));

% Torque at Mass Centre
Nc = sym(zeros(3,1,7));

% Force on Link Origin
Fo = sym(zeros(3,1,7));

% Torque at origin
No = sym(zeros(3,1,7));

% Joint Torques
T = sym(zeros(1,1,6));

% Angular Velocity
w = sym(zeros(3,1,7));
    w(1,1,1) = 0;
    w(2,1,1) = 0;
    w(3,1,1) = 0;

% Angular Acceleration
j = sym(zeros(3,1,7));
    j(1,1,1) = 0;
    j(2,1,1) = 0;
    j(3,1,1) = 0;

% Gravity
g = 9.81;

%Linear Acceleration **MODIFY FOR DIFFERENT SYSTEM IF NECESSARY**
Ao = sym(zeros(3,1,7));
    Ao(1,1,1)= 0;
    Ao(2,1,1)= -g;
    Ao(3,1,1)= 0;

% Positions of the Centre of Mass **MODIFY FOR DIFFERENT SYSTEM**
Pc = sym(zeros(3,1,7));
    Pc(:,:,1) = [0; 0; 0];
    Pc(:,:,2) = [0.0075 0.1425 0.0025];
    Pc(:,:,3) = [0.0075 0.1 0.0025];
    Pc(:,:,4) = [0; 0; 0];
    Pc(:,:,5) = [0; 0; 0];
    Pc(:,:,6) = [0; 0; 0];
    Pc(:,:,7) = [0; 0; 0];

% Masses **MODIFY FOR DIFFERENT SYSTEM**
m = sym(zeros(7,1));
    m(1,1) = 0;
    m(2,1) = 0.2;
```

```
    m(3,1) = 0.15;
    m(4,1) = 0;
    m(5,1) = 0;
    m(6,1) = 0;
    m(7,1) = 0;

%% Moment of Inertia Calculations
syms X Y Z
syms p % density
%p = 2800;

Ixx = sym(zeros(1,7));
Iyy = sym(zeros(1,7));
Izz = sym(zeros(1,7));
Ixy = sym(zeros(1,7));
Ixz = sym(zeros(1,7));
Iyz = sym(zeros(1,7));

for i = 1:7;
    Ixx(:,i) = int(int(int((Y^2 + Z^2)*p,Z,-Pc(3,1,i),Pc(3,1,i)),Y,-
Pc(2,1,i),Pc(2,1,i)),X,-Pc(1,1,i),Pc(1,1,i));
    Iyy(:,i) = int(int(int((X^2 + Z^2)*p,X,-Pc(1,1,i),Pc(1,1,i)),Z,-
Pc(3,1,i),Pc(3,1,i)),Y,-Pc(2,1,i),Pc(2,1,i));
    Izz(:,i) = int(int(int((X^2 + Y^2)*p,Y,-Pc(2,1,i),Pc(2,1,i)),X,-
Pc(1,1,i),Pc(1,1,i)),Z,-Pc(3,1,i),Pc(3,1,i));
end

for i = 1:7;
    Ixy(:,i) = -int(int(int(X*Y*p,Y,-Pc(2,1,i),Pc(2,1,i)),X,-
Pc(1,1,i),Pc(1,1,i)),Z,-Pc(3,1,i),Pc(3,1,i));
    Ixz(:,i) = -int(int(int(X*Z*p,X,-Pc(1,1,i),Pc(1,1,i)),Z,-
Pc(3,1,i),Pc(3,1,i)),Y,-Pc(2,1,i),Pc(2,1,i));
    Iyz(:,i) = -int(int(int(Y*Z*p,Z,-Pc(3,1,i),Pc(3,1,i)),Y,-
Pc(2,1,i),Pc(2,1,i)),X,-Pc(1,1,i),Pc(1,1,i));
end

% Inertia Matrix of Link about Centre of Mass
Ia = sym(zeros(3,3,7));

for i = 1:7;
    Ia(:,:,i) = [Ixx(:,i)  Ixy(:,i) Ixz(:,i); Ixy(:,i) Iyy(:,i)
Iyz(:,i); Ixz(:,i) Iyz(:,i) Izz(:,i)];
end

%% %%%%%%%%%%%%%%%%% Outwards Iterations %%%%%%%%%%%%%%%%%%%%%%%%%%

% Angular Velocities
for i = 1:6;
    w(:,:,i+1)= TM(1:3, 1:3, i).'*w(:,:,i)+A(i+1,1).*[0;0;1];
end

% Angular Accelerations
for i = 1:6;
    j(:,:,i+1) = TM(1:3, 1:3, i).'*j(:,:,i)+cross((TM(1:3, 1:3,
i).'*w(:,:,i)),(A(i+1,1).*[0;0;1]))+B(i+1,1).*[0;0;1];
end
```

```
% Origin Accelerations
for i = 1:6;
   Ao(:,:,i+1) = TM(1:3, 1:3,i)*(Ao(:,:,i) +
cross(j(:,:,i),TM(1:3,4,i)) +
cross(w(:,:,i),cross(w(:,:,i),TM(1:3,4,i))));
end

% Acceleration - COM
for i = 1:6;
   Ac(:,:,i+1) = Ao(:,:,i+1) + cross(j(:,:,i+1),Pc(:,:,i+1)) +
cross(w(:,:,i+1),cross(w(:,:,i+1),Pc(:,:,i+1)));
end

% Forces - COM
for i = 1:6;
   Fc(:,:,i+1) = m(i+1,1).*Ac(:,:,i+1);
end

% Torque - COM                        **CHANGE Ia to Ic IF NECESSARY**
for i = 1:6;
   Nc(:,:,i+1) = Ia(:,:, i+1)*j(:,:,i+1)+cross(w(:,:,i+1),Ia(:,:,
i+1)*j(:,:,i+1));
end

%% %%%%%%%%%%%%%%%%%% Inwards Iterations %%%%%%%%%%%%%%%%%%%%%%%%%%%%

% Force Balance
for i = 6;
   Fo(:,:,i)=Fc(:,:,i)+TM(1:3,1:3,i+1)*Fo(:,:,i+1);
end

for i = 5;
   Fo(:,:,i)=Fc(:,:,i)+TM(1:3,1:3,i+1)*Fo(:,:,i+1);
end

for i = 4;
   Fo(:,:,i)=Fc(:,:,i)+TM(1:3,1:3,i+1)*Fo(:,:,i+1);
end

for i = 3;
   Fo(:,:,i)=Fc(:,:,i)+TM(1:3,1:3,i+1)*Fo(:,:,i+1);
end

for i = 2;
   Fo(:,:,i)=Fc(:,:,i)+TM(1:3,1:3,i+1)*Fo(:,:,i+1);
end

for i = 1;
   Fo(:,:,i)=Fc(:,:,i)+TM(1:3,1:3,i+1)*Fo(:,:,i+1);
end

% Torque Balance
for i = 6;
   No(:,:,i) = Nc(:,:,i) + TM(1:3,1:3,i+1)*No(:,:,i+1) +
cross(Pc(:,:,i),Fc(:,:,i)) +
cross(TM(1:3,4,i+1),TM(1:3,1:3,i+1)*Fo(:,:,i+1));
end
```

```
for i = 5;
   No(:,:,i) = Nc(:,:,i) + TM(1:3,1:3,i+1)*No(:,:,i+1) +
cross(Pc(:,:,i),Fc(:,:,i)) +
cross(TM(1:3,4,i+1),TM(1:3,1:3,i+1)*Fo(:,:,i+1));
end

for i = 4;
   No(:,:,i) = Nc(:,:,i) + TM(1:3,1:3,i+1)*No(:,:,i+1) +
cross(Pc(:,:,i),Fc(:,:,i)) +
cross(TM(1:3,4,i+1),TM(1:3,1:3,i+1)*Fo(:,:,i+1));
end

for i = 3;
   No(:,:,i) = Nc(:,:,i) + TM(1:3,1:3,i+1)*No(:,:,i+1) +
cross(Pc(:,:,i),Fc(:,:,i)) +
cross(TM(1:3,4,i+1),TM(1:3,1:3,i+1)*Fo(:,:,i+1));
end

for i = 2;
   No(:,:,i) = Nc(:,:,i) + TM(1:3,1:3,i+1)*No(:,:,i+1) +
cross(Pc(:,:,i),Fc(:,:,i)) +
cross(TM(1:3,4,i+1),TM(1:3,1:3,i+1)*Fo(:,:,i+1));
end

for i = 1;
   No(:,:,i) = Nc(:,:,i) + TM(1:3,1:3,i+1)*No(:,:,i+1) +
cross(Pc(:,:,i),Fc(:,:,i)) +
cross(TM(1:3,4,i+1),TM(1:3,1:3,i+1)*Fo(:,:,i+1));
end


% Motors Inputs
for i = 1:7
   T(:,:,i) = No(:,:,i).'*[0 ;0; 1]; %Torque used due to rotation
only
end

%% Display
for i = 1:7
          disp(vpa(simplify(T(:,:,i)),3))
end

return
```

Appendix C – SimMechanics Link Procedure

Once the assembly has been modelled, use the SimMechanics Link plug-in in the Menu bar and select Export as SimMechanics First Generation.

Select the folder, and enter the filename you wish to save the file as.

Once the XML file has been exported, enter the following code into MATLAB® to import the files and begin the simulation.

```
% define the path to the file
path(path,'<folder directory.')
% import the CAD model into MATLAB
mech_import('filename.xml')
```

Once the simulation has been built, the schematic block diagram will be displayed.

Using the Simulink library add the necessary blocks in order to drive the simulation and record the results.

Further information on building a simulation can be found at
http://www.mathworks.co.uk/products/simulink/

Appendix D – Device Schematic Block Diagram

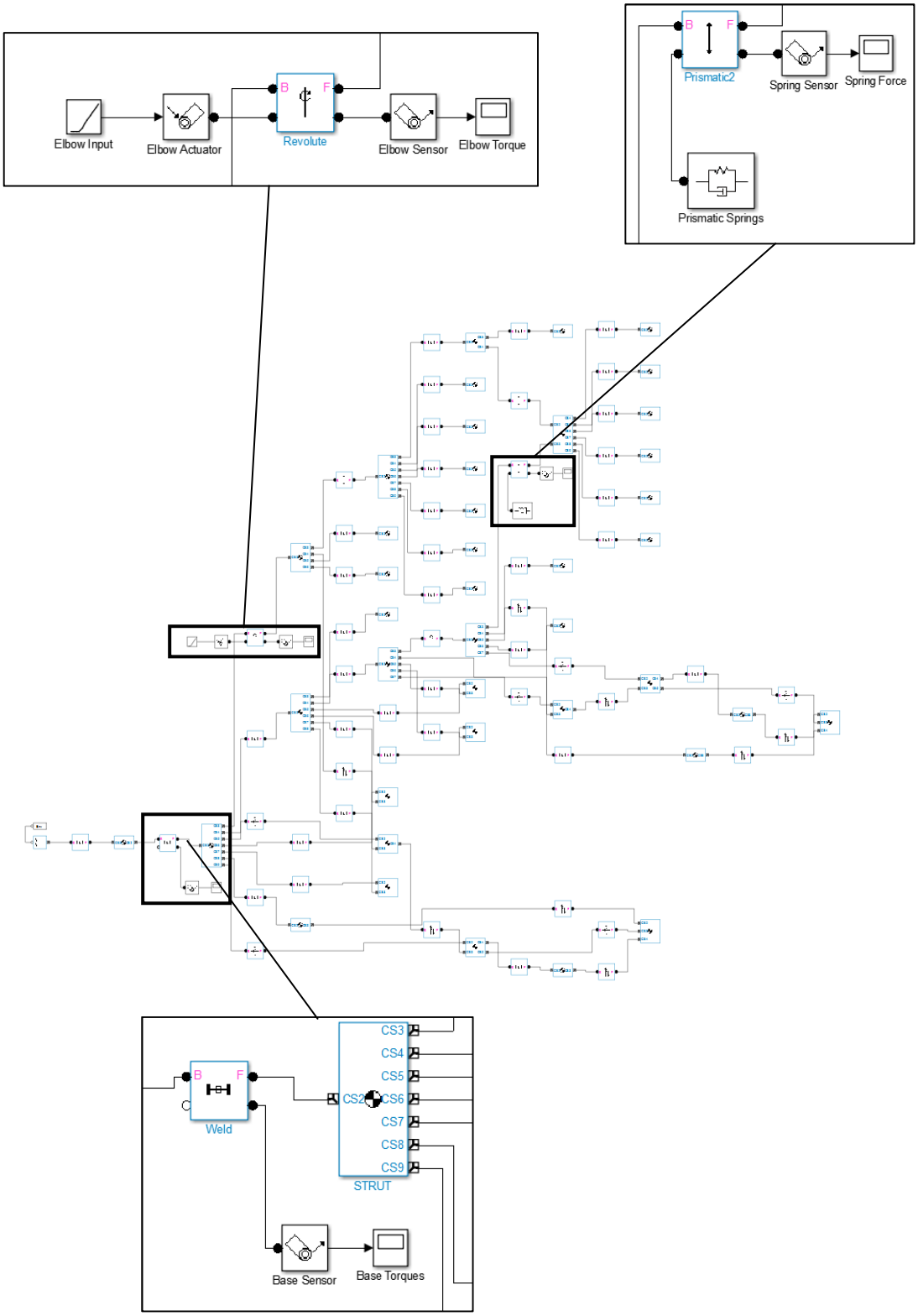

Figure 33: The schematic block diagram for the device, outlining key areas.

Appendix E – Permissions

IEEE

Requirements to be followed when using any portion (e.g., figure, graph, table, or textual material) of an IEEE copyrighted paper in a thesis:

1) In the case of textual material (e.g., using short quotes or referring to the work within these papers) users must give full credit to the original source (author, paper, publication) followed by the IEEE copyright line © 2011 IEEE.

2) In the case of illustrations or tabular material, we require that the copyright line © [Year of original publication] IEEE appear prominently with each reprinted figure and/or table.

3) If a substantial portion of the original paper is to be used, and if you are not the senior author, also obtain the senior author's approval.

Requirements to be followed when using an entire IEEE copyrighted paper in a thesis:

1) The following IEEE copyright/ credit notice should be placed prominently in the references: © [year of original publication] IEEE. Reprinted, with permission, from [author names, paper title, IEEE publication title, and month/year of publication]

2) Only the accepted version of an IEEE copyrighted paper can be used when posting the paper or your thesis on-line.

3) In placing the thesis on the author's university website, please display the following message in a prominent place on the website: In reference to IEEE copyrighted material which is used with permission in this thesis, the IEEE does not endorse any of [university/educational entity's name goes here]'s products or services.

Internal or personal use of this material is permitted. If interested in reprinting/republishing IEEE copyrighted material for advertising or promotional purposes or for creating new collective works for resale or redistribution, please go (link below) to learn how to obtain a License from RightsLink.

http://www.ieee.org/publications_standards/publications/rights/rights_link.html

If applicable, University Microfilms and/or ProQuest Library, or the Archives of Canada may supply single copies of the dissertation.

Cambridge University Press

Students can reuse an extract free of charge. Cambridge University Press grants a license for all orders, including $0 orders. Please select the Continue button and place an order for this reuse.

Wikimedia Commons